4 Molecular Genetics and Pathophysiology

Andrew O. M. Wilkie

Introduction

Few pediatric disorders are as readily clinically diagnosed as Apert syndrome. The combination of characteristic dysmorphic appearance accompanied by syndactyly of the hands and feet (usually in the absence of polydactyly) is shared with very few other conditions. There is correspondingly exquisite specificity in the underlying molecular genetic basis of Apert syndrome; all described mutations occur in a single gene, *FGFR2* (encoding fibroblast growth factor [FGF] receptor type 2), and > 98% of these can be attributed to one of two heterozygous amino acid substitutions, p.Ser252Trp or p.Pro253Arg, the "canonical" Apert syndrome missense mutations that map to adjacent positions of the polypeptide chain.

Alongside this apparently simple pattern, two seemingly paradoxical observations must be explained. First, many of the other 1–2% of Apert syndrome mutations are of a completely different nature from the missense variants, being either large deletions or insertions that affect a different region of *FGFR2* from the canonical substitutions. Second, the amino acid substitutions themselves must be exquisitely specific in their pathological mechanism, because other nearby missense variants (including at the Ser252 and Pro253 residues themselves) are not associated with Apert syndrome.

In fact, putting these observations together is central to understanding the pathophysiological processes underlying Apert syndrome. This chapter will describe how human molecular genetics, biochemistry, cell and structural biology, and mouse models have all played a key role in defining the mechanisms.

This work leads to two other topics explored in this chapter. The first is to explain why the apparent germline mutation rate in *FGFR2* causing the two canonical amino acid substitutions is so high (~1000-fold above background). In fact, the study of Apert syndrome *FGFR2* mutations provided key evidence for defining a newly described pathological phenomenon, termed selfish spermatogonial selection (SSS), to explain this. The second topic is to explore how knowledge of the mechanisms of abnormal signaling in Apert syndrome can help to pinpoint ways to counteract the harmful effects of the mutations on development—although achieving this therapeutically will have many challenges.

A. O. M. Wilkie (✉)
MRC Weatherall Institute of Molecular Medicine, University of Oxford, John Radcliffe Hospital, Headington, Oxford, UK

Oxford Craniofacial Unit, Oxford University Hospitals NHS Foundation Trust, John Radcliffe Hospital, Headington, Oxford, UK

Oxford Centre for Genomic Medicine, Oxford University Hospitals NHS Foundation Trust, Nuffield Orthopaedic Centre, Headington, Oxford, UK
e-mail: andrew.wilkie@imm.ox.ac.uk

J. G. Meara et al. (eds.), *Apert Syndrome*, https://doi.org/10.1007/978-3-032-12551-4_4

Discovery of Canonical *FGFR2* Mutations (p.Ser252Trp, p.Pro253Arg) in Apert Syndrome

By the early 1990s, geneticists were making good progress with mapping the human genome. Several important disease genes had already been found—for example those for Duchenne muscular dystrophy [54] and cystic fibrosis [74]. These successes had come either from identifying a chromosomal rearrangement visible down the microscope (such as a large deletion or translocation), which was postulated to directly disrupt the disease gene in question, or by tracking the disease through large families, enabling the position of the disease gene to be localized by linkage to polymorphic genetic markers. Key early highlights when applying these approaches in the craniofacial field came in 1991, when Greig cephalopolysyndactyly was solved (*GLI3* gene) using chromosome translocations [85], and in 1993, when a linkage and candidate gene approach was used to show that a large family segregating a dominantly inherited form of craniosynostosis ("Boston-type") harbored an amino acid substitution encoded by the *MSX2* gene [31].

For Apert syndrome, 1994 proved to be the key year. Late in 1993 the author had moved to Oxford, England, to join Sarah Slaney (now Smithson), a clinical fellow already working there, with the goal of discovering the genetic basis of Apert syndrome. Adopting one of the strategies described above, we checked the karyotypes of many dozens of individuals with Apert syndrome in the hope of identifying a rare patient harboring a visible chromosome abnormality (an entirely fruitless quest, as it turned out). In parallel, we searched for families in which an individual with Apert syndrome had two or more children (irrespective of whether they were affected or unaffected); this involved sending personal letters by airmail (email was only just becoming popular) to dozens of craniofacial surgeons around the world. The outcome was the identification of just three families (comprising four informative meioses), making feasible a screen of a small number of candidate loci to check whether the segregation of genetic markers transmitted from the affected parent to each of their children was concordant with the presence of the condition.

During 1994, scientific advances moved apace. In June, linkage studies in Crouzon syndrome, a dominantly inherited craniosynostosis disorder sharing similar facial features to Apert syndrome, localized the major Crouzon syndrome locus to the long arm of chromosome 10, where the *FGFR2* gene was known to reside (although this detail was not highlighted by the authors of the paper [68]). The following month, the first disorder caused by mutation in a fibroblast growth factor receptor was reported (achondroplasia with mutation in *FGFR3* [78]). By August 1994, the author's communication with the group working at the Institute of Child Health/Great Ormond Street Hospital, London, England (led by Susan Malcolm, William Reardon, and Robin Winter), confirmed that they had succeeded in identifying *FGFR2* mutations in Crouzon syndrome; this was reported in September 1994 [71].

These developments set the scene for the Oxford group to use samples from their four Apert syndrome meioses for candidate gene exclusion. Of the five genes chosen based on the previous discoveries—the two MSX genes *MSX1* and *MSX2*, and three of the four FGFR genes, *FGFR1*, *FGFR2*, *FGFR3*—four could be excluded based on inconsistent segregation patterns; only *FGFR2* showed consistent segregation, albeit there was a 1-in-16 probability this had occurred entirely by chance [91, 92]. This prompted an intensive search for mutations in the entire coding region of *FGFR2* in a panel of 40 samples from unrelated patients with Apert syndrome that had been collected by this stage. Essential to the success of this endeavor was the availability of fibroblast or lymphoblastoid cell lines from affected individuals, so that complementary DNA (cDNA)—as opposed to genomic DNA—could be screened for mutations. (At this point in time, the intronic sequences flanking the exons of *FGFR2* were not fully catalogued, so that other investigators were using genomic primers for polymerase chain reaction [PCR] designed from sequences at the ends of the exons. Because

both canonical Apert syndrome mutations turn out to reside within 10 base pairs of the start of an exon, any primer designed from the genomic DNA sequence would sit directly on top of the Apert syndrome mutations, rendering them physically impossible to detect.)

The first cloned cDNA sequence result pinpointing one of the Apert syndrome mutations in *FGFR2* (c.755C>G encoding the p.Ser252Trp amino acid substitution) is shown in Fig. 4.1a; the c.758C>G (p.Pro253Arg) substitution was identified during the following week. Of the first 40 unrelated samples analyzed, 25 were heterozygous for p.Ser252Trp and 15 for p.Pro253Arg [91, 92]. Indeed, subsequent studies from many different countries have confirmed the predominance of these two canonical mutations, which together account for >98% of patients with Apert syndrome (Table 4.1)—the p.Ser252Trp variant being about twice as common as p.Pro253Arg. Figure 4.1b shows the sequence context of the canonical mutations, located within the linker between the extracellular immunoglobulin-like (Ig) domains IgII and IgIII of FGFR2. Note that both mutations involve C>G transversions at the middle nucleotide of adjacent triplet codons; however, the Ser252 codon (TCG) contains a CG dinucleotide, which is potentially hypermutable [70], whereas the Pro253 codon (CCT) does not (substituted bases underlined). Although this could contribute to the greater prevalence of the Ser252Trp mutation, differential selection is likely to be quantitatively more important (see Section "Apert syndrome and selfish spermatogonial selection: experimental evidence and clinical implications").

To understand the mechanisms whereby just two mutations cause the great majority of cases of Apert syndrome, two questions regarding important pieces of contextual information are essential to answer. First, what is the structure of a fibroblast growth factor receptor (FGFR) and how does it function? Second, what differentiates Apert syndrome mutations from closely adjacent *FGFR2* mutations that, as had become apparent within a short space of time, cause two other classical craniosynostosis syndromes, Crouzon and Pfeiffer syndromes [32, 37, 71, 76]?

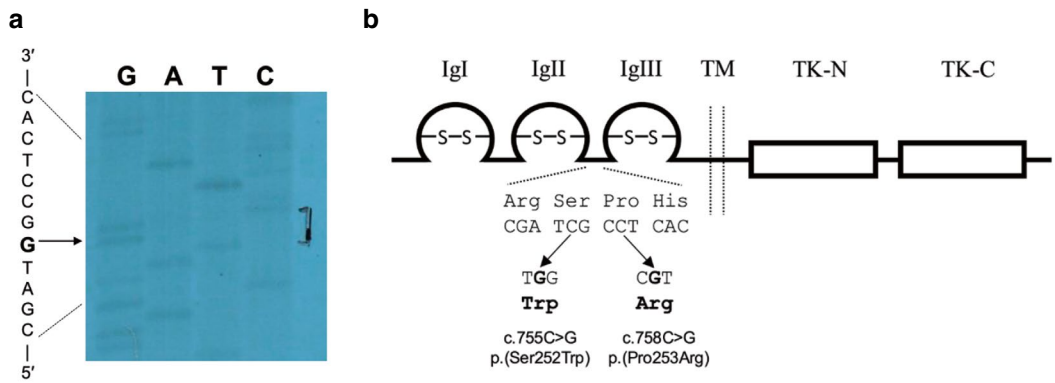

Fig. 4.1 The canonical Apert syndrome mutations in *FGFR2*. (**a**) The first autoradiographic evidence identifying a specific Apert syndrome mutation, which was obtained on September 27, 1994. Dideoxy-DNA sequencing of cloned *FGFR2* cDNA ("clone 73") was undertaken using ^{35}S-labeled dATP (deoxyadenosine triphosphate). The bracket mark is an annotation on the original autoradiograph highlighting the location of the variant nucleotide. Note how G (enlarged and bold in the sequence interpretation) replaces the expected C at this position. This individual has the 755C>G mutation. (**b**) Context of the canonical mutations. The FGFR2 protein comprises extracellular FGF-binding immunoglobulin-like domains (IgI, IgII, IgIII), each including a pair of buried, covalently linked cysteine residues (-S-S-), a single-pass transmembrane region (TM), and a split tyrosine kinase domain (TK-N and TK-C). The canonical Apert syndrome mutations 755C>G and 758C>G encode amino acid substitutions p.(Ser252Trp) and p.(Pro253Arg), respectively, located at adjacent amino acid residues in the linker between the IgII and IgIII domains

Table 4.1 Mutation spectrum in independent studies of Apert syndrome comprising ≥15 unrelated patients

Country of origin	c.755C>G (p.Ser252Trp)	c.758C>G (p.Pro253Arg)	Other mutations (total)	Total	References
UK + international	147	74	6	227	Bochukova et al. [7]
Australia	34	13	2[a]	47	Roscioli et al. [75]
USA	20	18		38	Fearon and Podner [14]
France	23	12	1	36	Lajeunie et al. [38]
USA	26	9	1[a]	35	Park et al. [63]
Brazil	16	10	1	27	Passos-Bueno et al. [65]
Spain	15	8		23	Paumard-Hernandez et al. [66]
Canada	13	3		16	Chun et al. [12]
Taiwan	13	2		15	Tsai et al. [84]
Norway	9	6		15	Tonne et al. [82]
Total	316 (66.0%)	155 (32.4%)	8 (1.7%)	479	

[a]These patients were also reported by Bochukova et al. [7], so are not separately included in the total

Biological and Pathological Context: FGFR2 Structure, Function, and Comparative Mutation Patterns in Apert, Crouzon, and Pfeiffer Syndromes

Some key molecular aspects of FGFR structure and function are illustrated in Fig. 4.2. As the name implies, the classical function of FGFRs (of which there are four major members) is to act as sensors for extracellular fibroblast growth factors (FGFs), which comprise 18 mostly paracrine-acting family members (reviewed by [62]). FGFR molecules traverse the cell membrane, so by detecting the prevailing extracellular FGF milieu they can signal into the cell to modify the cell's activity—for example, instructing it to divide, differentiate, or migrate, according to the particular intracellular pathways activated (reviewed by [16]).

As shown in the upper part of Fig. 4.2, in the presence of an appropriate paracrine FGF and heparan sulfate proteoglycans in the extracellular matrix, a binding complex is formed comprising two FGFs and two FGFRs; binding specificity is achieved through contacts made with the IgII and IgIII domains of the FGFR. This binding event brings the two FGFRs in close apposition, activating the intracellular tyrosine kinase domains through the cumulative phosphorylation of several key tyrosine residues [16]. As illustrated in the lower part of Fig. 4.2, either by phosphorylating other intracellular proteins or through the binding of proteins to the phosphotyrosines (for example Tyr766), several key intracellular signaling pathways (including RAS [rat sarcoma viral oncogene homolog]/MAP [mitogen activated protein] kinase, PI3K [phosphatidylinositol 3 kinase]/AKT [v-AKT murine thymoma viral oncogene homolog], and PKC [protein kinase C]) can be activated (reviewed by [8]). Set in this context, the potential significance of the canonical Apert syndrome substitutions can be appreciated, as they lie at adjacent positions in the linker between the IgII and IgIII domains (Fig. 4.1). This location suggests that they affect the affinity of FGF ligand binding [91, 92].

The second key context is to understand how Apert syndrome mutations differ in type and distribution compared to those causing Crouzon and Pfeiffer syndromes, the majority of which are located in the IgIII domain of FGFR2 just downstream of the canonical Apert syndrome mutations (Fig. 4.3). Like Apert syndrome, Crouzon and Pfeiffer syndromes are also characterized by craniosynostosis (although the pattern of suture fusions is more variable, with the sagittal suture commonly involved whereas there is a predilection for coronal synostosis in Apert syn-

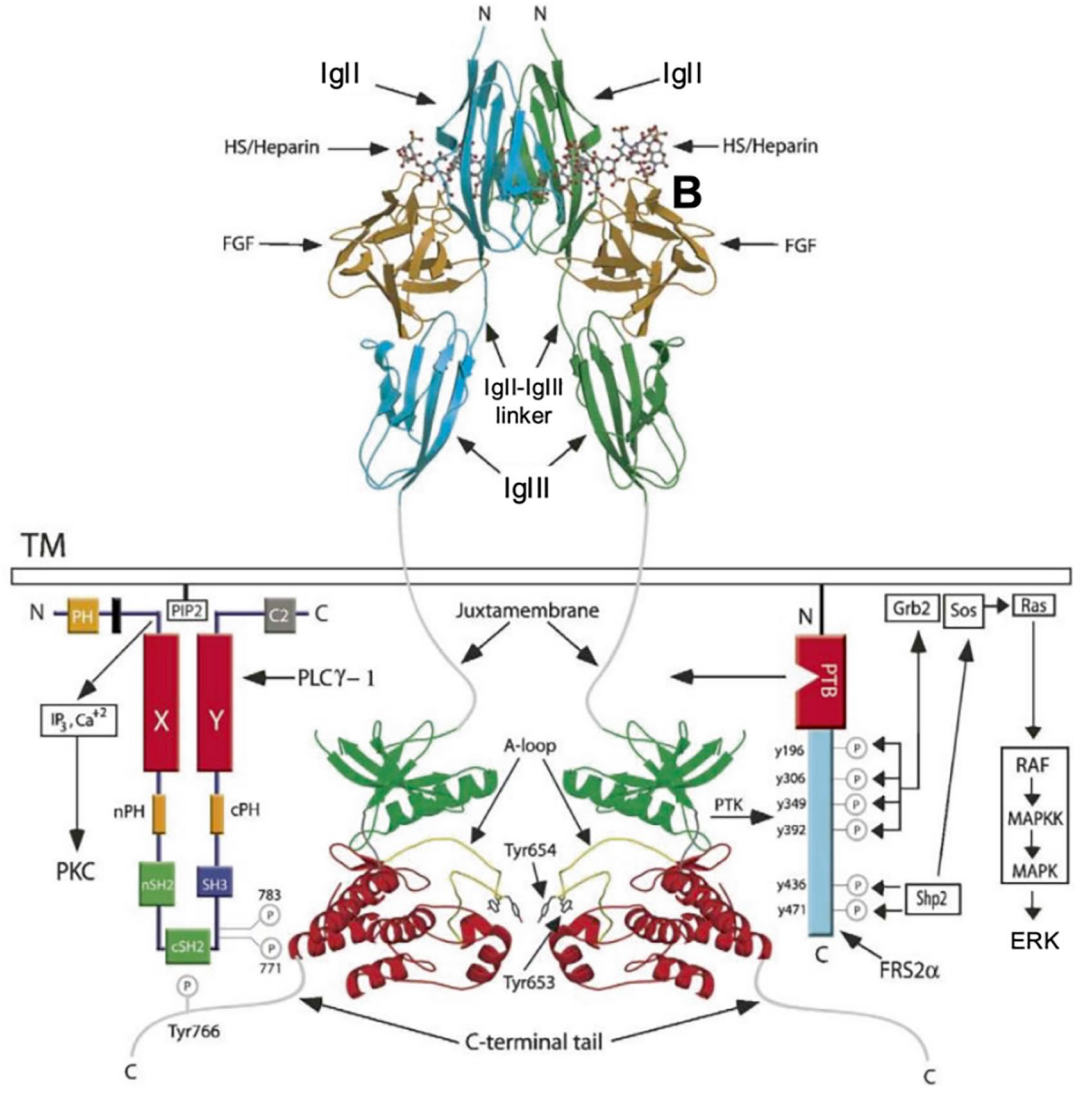

Fig. 4.2 Overview of the structural basis of FGF–FGFR signaling (reproduced in modified form from: [52]). The IgII and IgIII domains of two FGFR monomers (each colored blue or green) are shown in the upper part of the diagram binding to two FGFs (ochre), facilitated by heparan sulfate (HS) or heparin. After crossing the cell membrane (transmembrane, TM), juxtaposition of the two tyrosine kinase domains of the FGFRs promotes phosphorylation at key tyrosine residues (including those labeled Tyr653 and Tyr654), further activating the kinase activity to phosphorylate additional target proteins (denoted by P surrounded by circle). This leads to context-dependent activation of multiple intracellular pathways, including RAS/MAP kinase (MAPK), PKC, and PLCγ (phospholipase C gamma). See main text for further discussion

drome). However, the limb phenotype (by diagnostic definition) is different, varying from extensive cutaneous ± bony syndactyly in Apert syndrome, through broadening and medial deviation of the first digits (sometimes with incomplete cutaneous syndactyly) in Pfeiffer syndrome, to superficially normal limbs in Crouzon syndrome. In all three disorders, mutation hotspots are concentrated around two specific exons of *FGFR2*, exon IIIa and exon IIIc (Fig. 4.3). These exons together encode the IgIII domain; importantly however—and to further complicate mat-

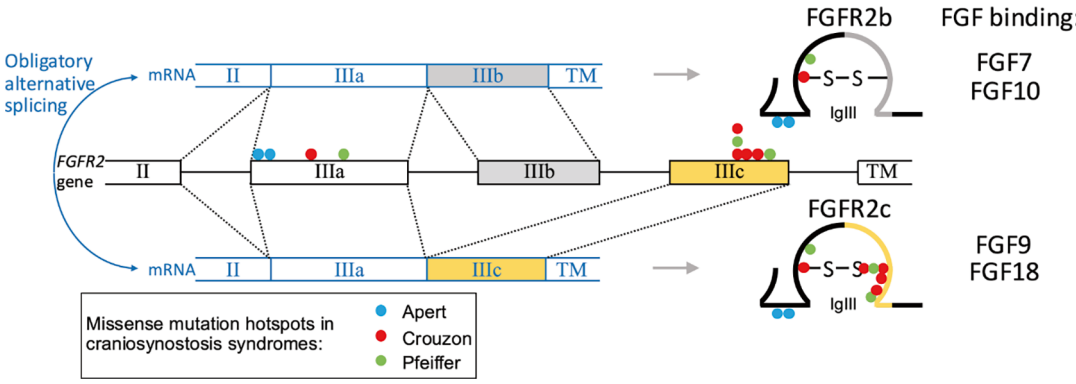

Fig. 4.3 Alternative splicing of *FGFR2* and location of mutation hotspots in craniosynostosis syndromes. A diagrammatic section of the *FGFR2* gene is shown (black type), with exons IgII, IgIIIa, IgIIIb, IgIIIc, and TM labeled and enclosed by boxes. Lines connecting exons are the intervening introns (not drawn to scale). Colored dots (see key) show locations of the ten most frequently occurring missense mutations causing Apert, Crouzon, and Pfeiffer syndromes in the gene and protein models (for clarity, omitted from mRNA models). Following initial transcription of *FGFR2*, developmentally regulated alternative splicing creates two different types of messenger RNA, shown in blue lettering above and below the gene model and depending on tissue-specific inclusion of either exon IIIb (gray) or exon IIIc (ochre). Translation yields two alternative isoforms of the FGFR2 protein termed FGFR2b and FGFR2c (right), which contain IgIII domains that differ in the sequence of the colored region (same coloring scheme as for mRNA) and bind a different repertoire of FGF ligands (only a selection of key ligands is shown). Note that although the canonical Apert syndrome mutations are present in both FGFR2 isoforms, a majority of Crouzon and Pfeiffer mutations are only expressed in the FGFR2c isoform

ters—an unusual obligatory alternative splicing event involving either the IIIc exon or the upstream IIIb exon creates two different forms of the receptor (FGFR2c and FGFR2b, respectively) that have different repertoires of FGF binding (see legend to Fig. 4.3 for further explanation). With some exceptions, the mechanisms by which Crouzon and Pfeiffer syndrome mutations act are qualitatively similar, but more severe quantitatively in Pfeiffer syndrome compared to Crouzon syndrome; hence the distribution and types of mutation overlap substantially between these two disorders. By contrast, Apert syndrome mutations are qualitatively distinct and belong to their own separate category.

A simple experiment, performed not long after the discovery of the molecular basis of Apert and Crouzon syndromes, illustrates the fundamentally contrasting mechanisms underlying the molecular pathology of these two disorders [4]. Isolated extracellular FGFR2 domains (ectodomains) containing wild-type (normal) sequence, the Apert syndrome substitution p. Ser252Trp, and a nearby substitution p.Ser267Pro associated with Crouzon syndrome (Fig. 4.4a) were electrophoresed in a non-denaturing gel in the presence or absence of FGF2, which normally binds to this extracellular region as illustrated in Fig. 4.2. Whereas the result for the Crouzon substitution was grossly abnormal (the mutant protein formed covalently cross-linked ectodomain dimers even in the absence of FGF2, and exhibited no binding to FGF2), the behavior of the Apert syndrome mutant protein was indistinguishable from wild-type (Fig. 4.4b). This shows that the Apert syndrome mutant retains the ability to bind FGF2 and, given the location of the substitutions in the IgII–IgIII linker, is predicted to affect binding affinity for specific FGF ligands. Indeed, this was demonstrated for a limited repertoire of FGFs by Anderson et al. [4]. In summary whereas Crouzon and Pfeiffer syndrome substitutions are mostly *constitutively* acting (meaning they cause FGFR2 activation in the absence of FGF ligand, often through the formation of FGFR2 dimer pairs that are covalently cross-linked by intermolecular cysteine-mediated disulfide bridges and thereby permanently activated; [73]), Apert syndrome mutations are *ligand-dependent*, exerting their pathology through a much more subtle mechanism. Although this answers the question, "why does

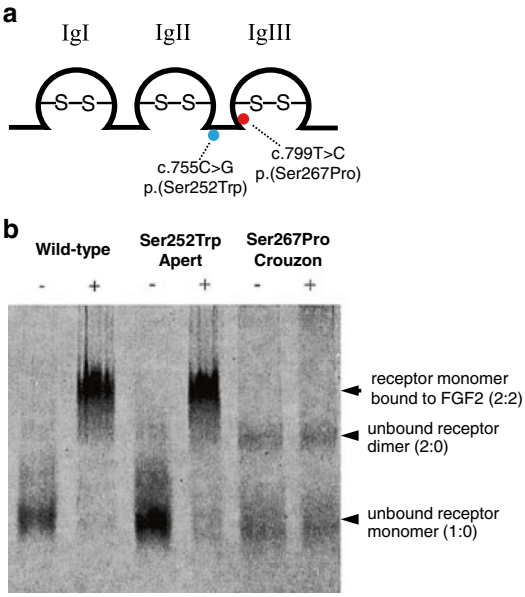

Fig. 4.4 FGF-binding experiment illustrating the fundamentally different nature of FGFR2 mutations causing Apert and Crouzon syndromes. (**a**) Design of the experiment, in which the extracellular part of FGFR2 only ("ectodomain," comprising IgI, IgII, IgIII domains) was synthesized, either in wild-type (normal) form, or containing one or other of the missense substitutions Ser252Trp (causing Apert syndrome) or Ser267Pro (causing Crouzon syndrome). (**b**) Result of non-denaturing polyacrylamide gel electrophoresis of FGFR2 ectodomains in either the absence (−) or presence (+) of a twofold molar excess of FGF2 ligand (reproduced in modified form from: [4]). Coomassie blue staining was used to visualize the protein. The interpretation is shown to the right of the gel, annotated with the ratio of protein species (ectodomain:FGF) present in each band visualized. See text for further commentary

Apert syndrome present differently from Crouzon and Pfeiffer syndromes, when their causative *FGFR2* amino acid substitutions are so close to each other?," it also leads to a new question: "What are the key FGF ligands mediating the Apert syndrome pathology?"

Canonical Substitutions p.Ser252Trp and p.Pro253Arg Result in Increased Binding Affinity and/or Altered Specificity for Specific FGFs

Two publications provided definitive data to explain how the canonical Apert syndrome mutations act in causing abnormal developmental signaling. First, Ibrahimi et al. [29] obtained structures by X-ray crystallography of the two Apert syndrome mutants bound to FGF2 (Fig. 4.5a). This work showed that both bulky amino acid substitutions introduce additional molecular contacts with the FGF, so they bind with higher affinity than normal (essentially, acting as "souped up" versions of the physiological receptor). The legend to Fig. 4.5a provides further details. Ibrahimi et al. [30] then exploited a biophysical method, surface plasmon resonance, to compare the binding affinities of every FGF to wild-type and Apert syndrome mutant receptors. A pathological effect in a given tissue and at a given time in development would be predicted if (i) the FGF ligand shows increased binding affinity to mutant receptor, compared to wild-type and (ii) the FGF ligand is expressed in that tissue. Table 4.2 summarizes the results for some of the ligand/receptor combinations thought to be most pathologically significant.

Perusal of Table 4.2 demonstrates two mechanisms (*increased affinity* and *altered specificity*) by which ligand-dependent Apert syndrome mutations could cause pathology; examples of each mechanism are shown in Fig. 4.5b. In the coronal suture (the most relevant cranial suture to consider in Apert syndrome), a combination of single cell transcriptomic analysis (which demonstrates expression of the relevant gene in the undifferentiated suture during embryogenesis) and mouse genetics (in which mutations of the cognate genes are associated with suture abnormalities) suggests that FGF9 and FGF18 are likely to be key physiological ligands [13, 27, 41, 58]. For both these ligands, the Apert syndrome mutants show enhanced FGF affinity (reflected in lower dissociation constant [K_D]) compared to wild-type FGFR2c, similar to the observation for FGF2 illustrated in the upper panel of Fig. 4.5b.

The effect on enhanced FGF9-mediated signaling is likely to be more important, for two reasons. First, the absolute K_D values are lower and fold-increase values are greater for FGF9 compared with FGF18 (especially for the p.Ser252Trp mutant; Table 4.2); second, for FGF9, the relative fold-increases in affinity, comparing the two mutations, align with the greater severity of the craniofacial phenotype associated with the p. Ser252Trp mutation (see Chap. 5), whereas for

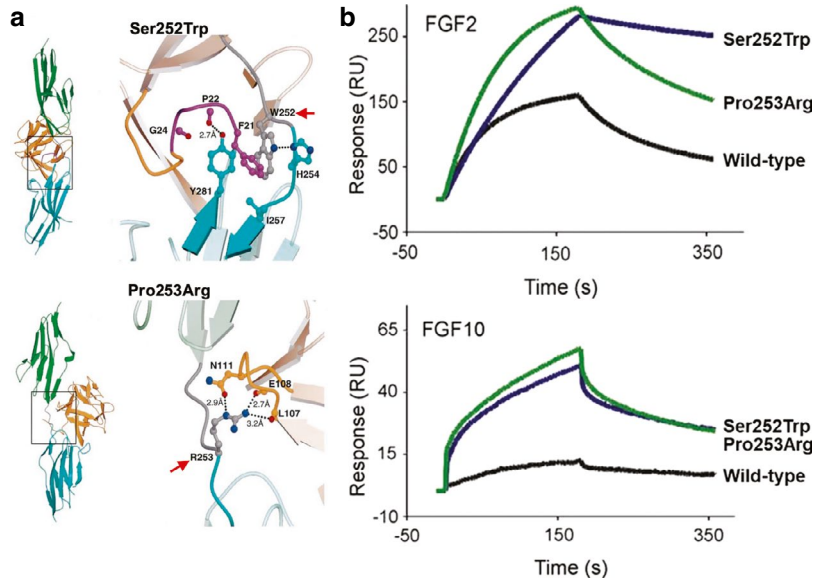

Fig. 4.5 Assessment of canonical Apert syndrome mutations using X-ray crystallography and surface plasmon resonance. (**a**) Structural basis by which canonical Apert syndrome mutations result in increased FGF ligand affinity (upper panel, Ser252Trp; lower panel, Pro253Arg). On the left is an overview of the IgII and IgIII domains (colored green and cyan, respectively) of Apert syndrome-mutant FGFR2c, bound to FGF2 (ochre). Rectangles indicate regions blown up in the images to the right. In the higher-resolution images, mutant residues in FGFR2 are highlighted with red arrows; note use of the single-letter amino acid abbreviation (W252 = Trp252, and R253 = Arg253). Both Apert syndrome mutations introduce additional contacts with FGF2, accounting for the increased binding affinity, but the mechanisms by which they do so are entirely distinct. The large aromatic side chain of Trp252 (gray) engages in a van der Waals (hydrophobic) interaction with the aromatic side chain of Phe21 in FGF2 (labeled F21 and colored purple). By contrast, the Arg253 side chain (gray) forms new hydrogen bonds with three different residues of FGF2, located at Leu107 [L107], Glu108 [E108] (both backbone interactions), and Asn111 [N111] (side chain interaction). Owing to these different mechanisms, the alteration in binding affinity for different FGFs by each Apert syndrome mutant is anticipated to be different (reproduced in modified form from: [29]). (**b**) Representative traces from surface plasmon resonance analysis of binding by FGF2 (above) and FGF10 (below) to wild-type (normal) and Apert syndrome mutants. The time trace shows the progressive binding of FGF to the receptor up to ~170 s, followed by washing off of the ligand. In the upper panel note how the FGFR2c-Ser252Trp mutant shows a very slow rate of FGF2 dissociation, consistent with increased binding affinity compared to wild-type. In the lower panel, the wild-type receptor exhibits almost no binding to FGF10, whereas both Apert syndrome mutants bind this ligand (altered ligand specificity). (Reproduced in modified form from: [52])

Table 4.2 Binding affinities of FGFR2 isoforms to selected FGF ligands[a]

Ligand	FGFR2 isoform	Wild-type	p.Ser252Trp		p.Pro253Arg		Relevant tissue
			K_D (M)	Fold increase	K_D (M)	Fold increase	
FGF2	FGFR2c	1.0×10^{-8}	2.2×10^{-9}	4.7	4.45×10^{-9}	2.3	Spermatogonial stem cell
FGF9	FGFR2c	1.3×10^{-6}	8.0×10^{-8}	15.8	1.0×10^{-7}	12.4	Cranial suture, spermatogonial stem cell
FGF18	FGFR2c	5.0×10^{-7}	1.8×10^{-7}	2.8	1.4×10^{-7}	3.5	Cranial suture
FGF10	FGFR2c	No binding	1.4×10^{-6}	NA[b]	9.4×10^{-7}	NA	Limb bud, cranial suture
FGF10	FGFR2b	6.2×10^{-7}	2.9×10^{-7}	2.1	4.0×10^{-7}	1.6	Limb bud

[a]Data reproduced from Ibrahimi et al. [30]; the lower the K_D (dissociation constant), the higher the binding affinity
[b]*NA* not applicable. Note that binding affinity for FGF10 is 1.5-fold higher for p.Pro253Arg compared to p.Ser252Trp

FGF18, the Pro253Arg substitution exhibits slightly greater fold-increase in affinity. In summary, the mechanism by which craniosynostosis occurs is likely to be through supraphysiological signaling in the cranial sutures, because of enhanced binding affinity of the Apert syndrome mutant receptors for ligands normally present in the suture. The strongest evidence that this effect is mediated through the FGFR2c rather than the FGFR2b isoform, is that many craniosynostosis-associated Crouzon and Pfeiffer syndrome mutations localize to exon IIIc and thereby exclusively affect the FGFR2c isoform (Fig. 4.3).

In the early limb bud, a different FGF signaling system is likely perturbed. Here, a key inductive signaling loop between mesenchymally located FGF10 and ectodermally located FGFR2b is normally essential for limb outgrowth, such that abolition of this signaling causes limblessness. That FGFR2b is clearly the key isoform for this signaling is demonstrated because FGFR2c is unable to bind FGF10 (Table 4.2, see wild-type column). Two publications [29, 30] demonstrated that when the FGFR2c isoform contains a canonical Apert syndrome mutation, it gains the ability to bind FGF10. This sets up a pathological autocrine signaling loop, because both FGFR2c and FGF10 are expressed in the mesenchymal cells of the limb bud (reviewed by [98]). Hence this pathology represents an ectopic or illegitimate signaling process. Although FGF10 binding affinity to Apert syndrome-mutant FGFR2b isoforms was found to be mildly enhanced (Table 4.2), evidence supporting that the syndactyly is FGFR2c-mediated includes: (i) the greater binding affinity of the FGFR2 Pro253Arg mutant, compared with Ser252Trp (Table 4.2), is consistent with the clinical observation that syndactyly tends to be more severe in association with the p.Pro253Arg mutation (see Chap. 5); and (ii) the observation [93] of syndactyly in two generations of a rare family harboring a p.[Ser252Leu;Ala315Ser] double substitution in *cis* on the same *FGFR2* allele (Table 4.3), which could only affect the FGFR2c isoform and was shown, like the canonical Apert syndrome mutations, to lead to illegitimate FGF10 binding. Relevant to understanding the mechanism of the double substitution, structural studies show that swapping Ala to Ser at position 315 switches FGFR2c to having FGFR2b-like binding properties [16, 30].

To end this section on a cautionary note, while the reductionist structural and biophysical methods presented above give satisfying explanations for the molecular pathology of Apert syndrome, by no means does this represent the full story. For example, Schuller et al. [77] and Ahmed et al. [1] used biochemical approaches to uncover several

Table 4.3 Additional molecular causes of Apert syndrome and closely related phenotypes

Category of mutation	DNA change	Amino acid change/Functional effect	References
Amino acid substitution	c.755_756delinsTT	p.Ser252Phe	Oldridge et al. [60]
	c.755_756delinsTT	p.Ser252Phe	Lajeunie et al. [38]
	c.755_756delinsTC	p.Ser252Phe	Goriely et al. [19]
	c.756_758delinsCTT	p.Pro253Phe	Lumaka et al. [42]
	c.[755C>T;943G>T]	p.[Ser252Leu;Ala315Ser][a]	Wilkie et al. [93]
Altered splicing (mostly *Alu* insertions)	c.940-4_940-3insAlu	Disrupted exon IIIc acceptor site	Oldridge et al. [61]
	c.1041_1042insAlu	[Disrupted exon IIIc splicing][b]	Oldridge et al. [61]
	c.1002_1003insAlu	[Disrupted exon IIIc splicing][b]	Bochukova et al. [7]
	c.940-19_940-18insAlu	[Disrupted exon IIIc acceptor site][b]	Topa et al. [83]
	c.940-2A>G[c]	Disrupted exon IIIc acceptor site (mild)	Passos-Bueno et al. [64]
Exon IIIc deletion	c.940-890_1084 + 895del	Complete loss of IgIIIc isoform	Bochukova et al. [7]
	c.940-1290_1021del	Hybrid IgIIIb/c isoform	Fenwick et al. [15]

[a]Syndactyly of hands and feet resembling Apert syndrome; broad forehead; no craniosynostosis
[b]Square brackets indicate predicted functional effect; no experimental data available
[c]Attenuated Apert syndrome phenotype with complete syndactyly of toes and syndactyly of digits 3 and 4 only in hands; patients with this mutation are more commonly diagnosed with Pfeiffer syndrome [61]

additional complexities in the cell biological effects of the canonical Apert syndrome mutations, notably showing that upon FGF9 stimulation, the mutant proteins persisted on the membrane of HEK (human embryonic kidney)-293 T cells in an abnormally glycosylated state, compared with the rapid endocytosis of the wild-type receptor on FGF stimulation. Qualitative differences in behavior between the Ser252Trp and Pro253Arg mutants were also documented [1, 77]. Another paradox—given the virtual ubiquity of FGFR2-mediated signaling for organogenesis in the early human embryo—is that these gain-of-function Apert syndrome mutations are compatible with life. This observation, and the lack of notably progressive natural history disease features in adults with Apert syndrome, both point to poorly understood mechanisms of tight autoregulation of FGF signaling that succeed in keeping in check the harmful effects of these mutations, in most cellular and developmental contexts.

Beyond the Canonical Mutations: Rare Molecular Causes of Apert Syndrome

In every 1–2 of 100 individuals with Apert syndrome, testing for the two common mutations yields negative results (Table 4.1). In all cases reported to date, a different molecular abnormality within the *FGFR2* gene has been identified (Table 4.3). These abnormalities can be divided into three broad groups: (1) amino acid substitutions, (2) variants (mostly insertions of *Alu* repeat sequences) causing altered splicing, and (3) deletions. These different types of molecular lesion are mapped onto the *FGFR2* gene in Fig. 4.6.

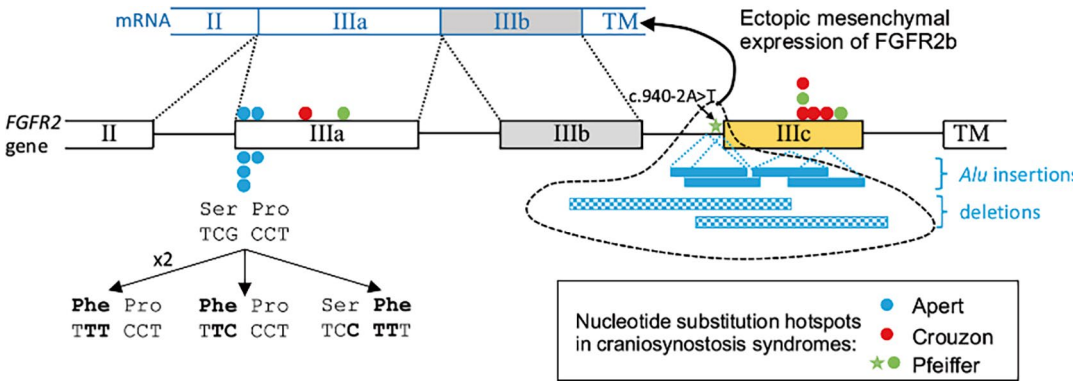

Fig. 4.6 Rare *FGFR2* mutations causing Apert syndrome. The gene model, showing part of *FGFR2* with hotspots of pathogenic missense mutation (filled circles above the gene; see key for color code—the two blue circles represent canonical Apert syndrome mutations), is reproduced from Fig. 4.3. Below the gene model are shown the positions of rare mutations causing Apert syndrome (see Table 4.3 for references). These fall into three classes: (1) (Four blue circles) Rare multinucleotide substitutions (bold type) involving two or three consecutive nucleotides ($n = 4$ cases) that normally encode the Ser252-Pro253 dipeptide; each results in substitution to a bulky phenylalanine (Phe) residue (2). (Four solid blue horizontal bars; dots connect to respective insertion sites) Insertions of mobile *Alu* genetic elements either within ($n = 2$), or immediately upstream of ($n = 2$) exon IIIc. Note that this diagram is not drawn to scale and that the inserted *Alu* elements (size range 214–368 base pairs) are all larger than the IIIc exon itself (145 base pairs) (3). (Two hatched blue bars) Deletions that either create a hybrid IIIb/IIIc exon (upper) or excise the IIIc exon entirely (lower). *Alu* insertions and deletions both functionally eliminate exon IIIc and result in the illegitimate expression of the IIIb exon-containing spliceform in mesenchymal tissues. Also indicated (green star) is the location of the c.940-2A>T mutation usually associated with Pfeiffer syndrome; see text for further details

Non-canonical Amino Acid Substitutions

The explanation for the rarity of the two different non-canonical Apert syndrome-causing amino acid substitutions (p.Ser252Phe and p.Pro253Phe) is straightforward. Each occurs within the same Ser-Pro dipeptide as the canonical substitutions and each encodes a substitution to phenylalanine (Phe), which has a bulky aromatic side chain. It is anticipated (but has not, to the author's knowledge, been experimentally established) that the Phe side chain would make additional contacts with FGF, analogous to those shown in Fig. 4.5a for the two canonical substitutions. The rarity of these events is attributable to the fact that conversion of both the Ser252 and Pro253 codons to Phe requires two bases of the codon to be substituted, an intrinsically rare event. It is important to note that Apert syndrome is not the inevitable consequence of amino acid substitution at this Ser-Pro dipeptide. Notably, p.Ser252Leu (resulting from c.934C > T) occurs at a low frequency in the normal population (1 in every 24,814 alleles in the gnomADv4.1.0 database; [34]) and—although rarely—heterozygous individuals may present with a mild form of Crouzon syndrome [59, 60]. Also, the p.Pro253Leu substitution has been reported in two patients with bicoronal synostosis [75].

Insertions and Deletions

The two other types of mutational event are much more surprising, both because they are completely different in nature (rearrangements involving *Alu* insertions, or deletions, between them varying in size between 214 bp and 1930 bp), and because they involve a different exon, exon IIIc, compared with exon IIIa where all the Apert syndrome-associated missense mutations localize (Table 4.3). As noted previously, exon IIIc contains multiple missense mutation hotspots, but these give rise to Crouzon and Pfeiffer syndrome phenotypes, not to Apert syndrome (see Figs. 4.3 and 4.6).

Although it has only been possible to perform functional analysis on samples from one of the patients harboring an *Alu* insertion, this provides a strong clue to the likely pathogenic mechanism. A skin biopsy from a patient with Apert syndrome heterozygous for a 368 bp *Alu* insertion (located three nucleotides upstream of the exon IIIc splice acceptor site) was cultured to yield keratinocytes (which normally express only the *FGFR2b* spliceform) and fibroblasts (which normally express only the *FGFR2c* spliceform). Whereas the keratinocytes maintained their expected expression pattern, the fibroblasts showed illegitimate expression of *FGFR2b* [61]. This is likely to reflect failure to recognize the exon IIIc splice acceptor, causing breakdown of the normal tissue-specific splice choice between exon IIIb and IIIc and leading to ectopic *FGFR2b* expression in tissues of mesenchymal origin (such as fibroblasts). A similar pathological process has most likely occurred in the other patients with *Alu* insertions. Meanwhile the two deletions, by definition, destroy the normal IIIb/IIIc splice site choice, therefore also driving the illegitimate mesenchymal expression either of the IIIb exon (patient with complete deletion of IIIc exon), or a IIIb/IIIc hybrid (patient with deletion bridging IIIb and IIIc exons). Although no corroborative functional studies were performed in either of the patients with Apert syndrome harboring deletions, cDNA analysis of a mouse model engineered to contain a complete deletion of exon IIIc ($Fgfr2^{\Delta IIIc/+}$; further discussed in Section "Mouse models of Apert syndrome") demonstrated that illegitimate expression of the IIIb spliceform indeed occurred in E14.5 whole mouse brains, which normally express the IIIc spliceform [21, 22].

The ectopic mesenchymal expression of the FGFR2b receptor isoform is anticipated to give rise to an autocrine signaling loop driven by FGF10 binding, which is analogous to the autocrine loop generated by FGFR2c isoforms bearing canonical Apert syndrome substitutions that illegitimately bind FGF10 [98]. This provides a neat explanation for how such very different underlying genetic lesions in *FGFR2* each cause

the Apert syndrome phenotype. By crossing the exon IIIc-deleted mouse strain, which develops craniosynostosis, with another strain in which the *Fgf10* gene was deleted, Hajihosseini et al. [22] found that in double mutants (*Fgfr2*$^{\Delta IIIc/+}$*; Fgf10*$^{-/-}$), normal cranial suture development was restored. In addition, most *Fgfr2*$^{\Delta IIIc/+}$ and *Fgf10*$^{+/-}$ mice exhibited amelioration of the abnormal lung lobulation, alveologenesis, and intersternebral cartilage ossification defects usually present in *Fgfr2*$^{\Delta IIIc/+}$ animals with a normal *Fgf10* genotype. It is therefore likely that in humans, illegitimate FGF10-mediated signal activation underlies craniosynostosis in patients with *Alu* insertions and exon IIIc deletions. By extension of this argument, abnormal FGF10-mediated signaling (as well as FGF9- and FGF18-mediated signaling discussed in Section "Canonical substitutions p.Ser252Trp and p.Pro253Arg result in increased binding affinity and/or altered specificity for specific FGFs") may contribute to craniosynostosis caused by the canonical mutations as well.

A final point to note is that some patients with Pfeiffer syndrome present with cutaneous syndactyly and that this may overlap phenotypically with some individuals with Apert syndrome who have particularly mild syndactyly. For example, Passos-Bueno et al. [64] reported a patient with a diagnostic label of Apert syndrome based on a combination of craniosynostosis, broad thumbs, cutaneous syndactyly of digits 3–4 in the hands, duplication of metatarsal 1 with fusion of the proximal phalanges and absence of the distal phalanges, and complete syndactyly of toes 2–5 in the feet. This individual was heterozygous for the mutation c.940-2A>G, located within the invariant acceptor splice site sequence of exon IIIc and co-located with c.940-2A>T, a mutation hotspot for Pfeiffer syndrome (Fig. 4.6, green starred variant). Indeed, the limb involvement of Pfeiffer syndrome patients with mutations of this splice site tends to be particularly severe and a previous study of two such patients (one each with c.940-2A>G and c.940-2A>T) demonstrated illegitimate expression of the *FGFR2b* spliceform in fibroblasts, that was similar to, but quantitatively less marked than, the patient with Apert syndrome with an *Alu* insertion analyzed in the same publication [61]. Hence the pathogenesis of this particular subtype of Pfeiffer syndrome may be viewed as qualitatively overlapping, but quantitatively less severe, than patients with Apert syndrome caused by *Alu* insertions or deletions involving exon IIIc.

Apert Syndrome and Selfish Spermatogonial Selection: Experimental Evidence and Clinical Implications

The reasons that this entire book is devoted to Apert syndrome are twofold. First, as a multisystem disorder, its clinical management poses many challenges and second, it is one of the most common syndromic causes of craniosynostosis. The multisystem presentation can be attributed to the importance of FGFR2 signaling in many organ systems (developmental pleiotropy). But why is Apert syndrome so common? Birth prevalence studies indicate a frequency of Apert syndrome of ~13.5 per million ([88]; also Chap. 5); nearly all of these cases are the result of new mutation. Given this frequency, what makes Apert syndrome remarkable is the very narrow mutational spectrum, with 98–99% cases accounted for by just two mutations in the human genome, occurring at a ~ 2:1 ratio. This means that the birth prevalence of the c.755C > G mutation is ~1 in 111,000 and the c.758C > G mutation is ~1 in 222,000, per diploid genome. If these figures are contrasted with the background per-allele germline mutation rate of 1.2×10^{-8} (~1 in 83,000,000; [5]), then the rates of the Apert syndrome mutations are elevated several hundred-fold above expectation and occur more frequently than any other de novo mutation in *FGFR2* [17, 33, 46]. The search for the underlying explanation for this remarkable mutation enrichment has led to the identification of a novel genetic phenomenon termed *selfish spermatogonial selection* (SSS; [17]). In fact, this turns out to be another manifestation of the developmental pleiotropy of FGFR2: in the context of a male germ cell, a mutation harmful to

the whole organism paradoxically confers a selective advantage to the particular testis cell in which it has randomly arisen.

Experimental Evidence for Selfish Spermatogonial Selection

The elucidation of SSS in Apert syndrome arose from four sequential discoveries that are summarized below and illustrated in Fig. 4.7. First, following the identification of the canonical *FGFR2* mutations causing Apert syndrome, a method was designed to determine, in each affected child/unaffected parent trio, whether the *FGFR2* allele on which the child's Apert syndrome mutation had arisen was the allele transmitted from the mother or the father. This method exploited two common natural variants (single nucleotide polymorphisms or SNPs) in *FGFR2* located within a few hundred base pairs of the Apert syndrome mutations, that could be phased with respect to the mutation and then tracked back to the parents to determine who had transmitted the allele bearing the mutation (see Fig. 4.7a and legend for details). This yielded the striking result that, in all 57 informative families, the mutant allele arose from the healthy father [53]. Relevant to this finding was the previous observation that the parents of children with Apert syndrome tended to be older than average for the population, and this effect appeared stronger for the father's age than the mother's age ([6, 72]; see also Chap. 5). The observation of exclusive paternal origin of Apert syndrome mutations [53], which at the time of writing this chapter remains the largest such study published for any genetic disorder, showed that to investigate the phenomenon of the high apparent mutation rate, it was necessary to develop methods to accurately measure levels of Apert syndrome mutations in men's sperm.

A robust method to measure the level of the more common *FGFR2* 755C > G Apert syndrome mutant molecule down to 1 in one million (based on digesting away the majority of the normal DNA using a restriction enzyme cutting the normal sequence, then quantifying the remaining material using pyrosequencing) was published by Goriely et al. [18]. This work, which studied 99 sperm donors and 6 additional men who had fathered a child with Apert syndrome, reported several key observations (Fig. 4.7b): (1) the 755C>G mutation was detectable in the sperm of a majority (but not all) men, with levels varying considerably from 1 in 6250 to less than 1 in a million; (2) the level in an individual man remained stable over weeks or months, indicating that the mutation source(s) were long-lived cells; (3) levels in sperm of fathers of children with Apert syndrome fell within the envelope of values found in other sperm donors, but tended to cluster in the upper part of the range (>1 in 10^5); and (4) levels of 755G mutant molecules in sperm were strongly positively correlated (r = 0.39) with the age of the donor. An additional unexpected observation, which exploited one of the nearby SNPs mentioned above (rs2071616) to distinguish the two *FGFR2* alleles, was that even in men producing relatively high levels of the Apert syndrome mutation in their sperm, the mutant alleles tended to predominate on just one or other of the two allelic copies, rather than being distributed ~50:50 between them. This key observation suggested that the originating mutations must be rare, but by conferring a selective (growth) advantage to the mutant cell, the cell's progeny become gradually more numerous over the course of time [18].

A prediction of the selective advantage model was that the originating mutations in the testis should be clonal, and hence potentially localized to small regions within a testis. Qin et al. [69] assessed this prediction for the c.755C > G mutation by cutting testis slices from cadaveric donors into ~200 pieces, measuring the level of c.755G in each piece, then constructing a three-dimensional heat map of mutant distribution based on these measurements [69]. This work showed that the Apert syndrome mutations within a given testis indeed tended to be highly localized, with the highest mutant level measured in an individual piece up to 6%, but also with large "deserts" of entirely mutation-negative regions between these hotspots ([69]; Fig. 4.7c). The same group subsequently made similar observations on the distribution of *FGFR2* c.758C>G

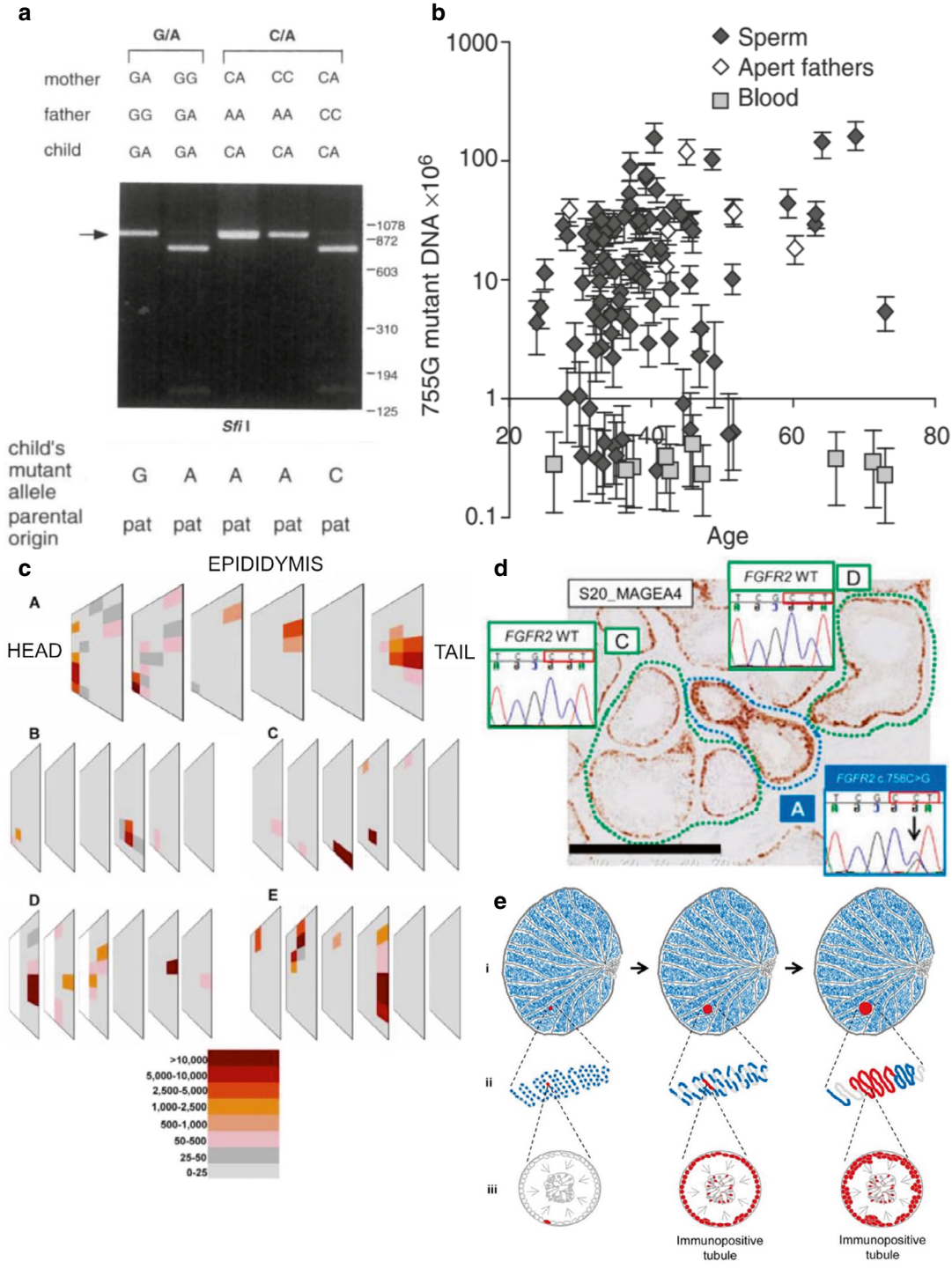
a
G/A
C/A
mother GA GG CA CC CA
father GG GA AA AA CC
child GA GA CA CA CA
1078
872
603
310
194
125
Sfi I
child's mutant allele G A A A C
parental origin pat pat pat pat pat
b
Sperm
Apert fathers
Blood
755G mutant DNA ×10^6
1000
100
10
1
0.1
20
40
60
80
Age
c
EPIDIDYMIS
HEAD
TAIL
A
B
C
D
E
>10,000
5,000-10,000
2,500-5,000
1,000-2,500
500-1,000
50-500
25-50
0-25
d
S20_MAGEA4
FGFR2 WT
C
FGFR2 WT
D
FGFR2 c.758C>G
A
e
i
ii
iii
Immunopositive tubule
Immunopositive tubule

Fig. 4.7 How the study of Apert syndrome mutations supports the theory of selfish spermatogonial selection. (**a**) Apert syndrome mutations arise exclusively on the *FGFR2* allele transmitted from the father. The top panel shows, for five different Apert syndrome trios (in each of which the child is heterozygous at c.755C>G and the parents are unaffected), the genotypes at one or other of two nearby polymorphic loci—rs2071616 (c.749-112G>A; labelled G/A) or rs2981451 (c.939+579C>A; labelled C/A). In the middle panel, allele-specific PCR was performed on the child's sample using primers designed selectively to amplify the A allele only (G/A variant), or the C allele only (C/A variant). The restriction enzyme *Sfi*I specifically digests the c.755G mutant allele; so if the product digested (yielding a shortened band on electrophoresis), this would indicate that mutant allele had been amplified, and vice-versa. The bottom panel shows the interpretation of the digest result, indicating the allele on which the Apert syndrome mutation must be present. In all cases displayed, the mutation is paternal (pat) in origin; this proved to be the case in all 57 informative families (figure from: [53]). (**b**) Quantitation of the 755C > G Apert syndrome mutation in sperm and blood samples (see key) in relation to age of the donor. Sperm measurements were obtained for 99 men with no family history of Apert syndrome and for 6 men who had fathered a child with Apert syndrome. Note that the mutations are effectively undetectable ($<10^{-6}$) in blood, but are present at measurable levels in sperm of most, but not all men in the population. See text for further discussion (figure from: [18]). (**c**) Spatial analysis of the c.755C > G mutation in four cadaveric testes from two men aged 54 and 62 years, obtained from a tissue bank (C and D are from different parts of the same testis). Each testis was dissected into ≥192 geographically registered pieces, the level of Apert syndrome mutation measured in each piece, and the distribution of mutations reconstructed for each testis according to the position of each piece in the original dissection. The color scale indicates the number of mutant molecules per million genomes (figure from: [69]). (**d**) Direct isolation and identification of an Apert syndrome mutation in a seminiferous tubule. Immunohistochemistry was performed on a testis cross-section with the antibody MAGEA4. Note the stronger peripheral brown staining in the tubule surrounded by blue dotted lines, compared to the tubules surrounded by green dotted lines. Insets show the results of *FGFR2* DNA sequencing of each of the highlighted regions, following microdissection of the corresponding tubule(s) from an adjacent tissue slice. The blue-surrounded tubule labeled A contains the c.758C > G Apert syndrome mutation (indicated by down-pointing arrow), whereas the green-surrounded tubules labeled C and D show only the normal *FGFR2* sequence at this location. Black scale bar indicates 500 μm (figure from: [45]). (**e**) Cartoon illustrating the evolution of a positively selected clone within the testis. Each figure part shows a whole testis at the top, a length of seminiferous tubule in the middle, and a cross-section through an individual seminiferous tubule at the bottom. Mutant cells are colored red. Left: A mutation has randomly arisen in a single spermatogonial stem cell, located adjacent to the basement membrane of the tubule. Middle and right: As a result of preferential proliferation of the cell and its progeny, the mutant cell has first populated the entire circumference of the tubule, then over the course of time the clone has extended along an increasing length of the tubule. Half the sperm produced by the mutant stem cell bear the Apert syndrome mutation, hence the output of mutant sperm increases over the years. Note that the absolute mutation level (hence the recurrence risk for the father) remains very low (<1 in 1000), because mutant cells only constitute a small fraction of the testis as a whole. (Figure from: [44])

mutations within the testis [11], as well as measuring levels of both mutations in sperm samples [96], independently concluding that their data best fitted a selective advantage rather than a mutation hotspot model.

Although these reports supported the occurrence of selective advantage, the underlying evidence for the cellular distribution of mutations was lost because the experimental approach used DNA extracted from testis pieces. Following the discovery [40] that immunohistochemistry on testis sections using an antibody raised to a tumor antigen (MAGEA4 [melanoma antigen gene A4]) highlighted a subset of seminiferous tubules exhibiting an abnormally prominent staining pattern, Maher et al. [45] then used a combination of laser capture microdissection, whole genome amplification of extracted DNA, and next-generation sequencing and targeted dideoxy-sequencing to demonstrate that these unusual-appearing tubules often harbored a specific mutation encoding a gain-of-function protein encoded by one or other of a handful of genes, including *FGFR2* [45]. Indeed, one of the mutations identified [45] was the Apert syndrome *FGFR2* c.758C > G, pinpointed in a seminiferous tubule from a 39-year-old man, whose testis had been removed as part of a hernia operation (Fig. 4.7d). Using cartoon illustrations of a testis, Fig. 4.7e summarizes the conclusions arising from this body of work, showing how, through a process of positive selection, a single cell harboring a rare, randomly occurring mutation forms a slowly expanding clone over the course of time. The process is referred to as "selfish," because although the mutation benefits the spermatogo-

nial stem cell in which it arises (conferring a replicative advantage), it is harmful to any progeny arising from fertilization by progeny mutant sperm (in this case, causing Apert syndrome). Further work has highlighted activation of RAS–MAP kinase, one of the key pathways activated by FGFR2 signaling (Fig. 4.2) as the common thread linking all the major genes for which mutations are enriched by selfish selection [46]. This provides evidence that the RAS–MAP kinase pathway plays a key role in regulating spermatogonial stem cell turnover; we will return to the important role of this pathway in Apert syndrome pathogenesis in Section "Pathways activated in Apert syndrome and approaches to therapeutic inhibition."

The cellular mechanisms of Apert syndrome-mediated selfish spermatogonial selection were investigated by Martin et al. [47] using mouse spermatogonial stem cells transduced with either the Apert syndrome FGFR2-Ser252Trp or wild-type cDNAs using a lentiviral system [47]. Confirming previous work, *FGFR2* was shown to be expressed in putative spermatogonial stem cells adjacent to the basement membrane of the seminiferous tubule. Apert syndrome-mutant cells showed increased proliferation when exposed to low doses of FGF2. Most pertinently, transplantation of labeled mutant or wild-type cells into mouse testes showed preferential population by the mutant cells, consistent with a selective advantage. Several FGFs appear to play physiological roles in the testis including FGF2, FGF5, FGF8, and FGF9, with cells responding to precise doses [36, 94]. Since the Apert syndrome mutations exhibit increased binding to most of these ligands [30], the strong selective advantage might work through a combinatorial effect involving several ligands.

Given the conclusion that, in the appropriate cellular context, an Apert syndrome mutation confers the cell with a proliferative advantage over its wild-type neighbors, it should not come as a surprise that the identical canonical mutations, when arising somatically in specific tissue types, have been identified in several cancers. In fact, the p.Ser252Trp FGFR2 mutation is the single most common somatic mutation occurring in endometrial cancer [67], and the COSMIC database documents the occurrence of the somatic equivalent of Apert syndrome mutations in other cancer types (https://cancer.sanger.ac.uk/cosmic/gene/analysis?ln=FGFR2). While a detailed discussion is outside the scope of this chapter, it is important to note that no strong evidence exists that Apert syndrome itself is associated with a substantially increased cancer risk. This seemingly paradoxical fact may be understood when it is appreciated that the milieu of the Apert syndrome-mutant cell differs according to context. In Apert syndrome itself, all neighboring cells are also mutant, whereas in cancer (as well as in men's testes), the neighboring cells are wild-type, making it more likely in the latter situation that differential selection between cells can occur.

Clinical Implications of Selfish Spermatogonial Selection

An important clinical implication of this body of work is that when a healthy couple has a child affected by Apert syndrome, the recurrence risk for another affected child is likely to be extremely low (< 1 in 1000; [90]). This is because, even though the mutant clone is positively selected (explaining the high mutation rate), it remains diluted out by the large number of non-mutant cells in the entire testis (as illustrated in Fig. 4.7e). This deduction is further supported by quantitation of Apert syndrome mutation levels in individuals who have fathered a child with Apert syndrome (Fig. 4.7b). While high-level germinal mosaicism is theoretically possible, and has been documented in a single instance of a Crouzon *FGFR2* mutation [20], it has not yet been molecularly confirmed in Apert syndrome, although a single sibling recurrence was reported in the historical literature [3]. Owing to this very low recurrence risk it is the author's recommendation, for couples who have had a child affected with Apert syndrome, not to promote use of invasive diagnostic procedures in subsequent pregnancies, as the risk of causing the miscarriage of an unaffected fetus will in nearly all cases exceed the risk of Apert syndrome itself.

An alternative route for the genetic detection of Apert syndrome fetuses during pregnancy is to exploit the fact that small amounts of fetal DNA circulate in the maternal blood. This has led to development of a generalized strategy for non-invasive prenatal screening (NIPS) including multiple genetic disorders, starting with a maternal peripheral blood sample [99]. Among the proof-of-principle cases presented in this series was the confirmation of Apert syndrome in a pregnancy of 20 weeks' gestation, already clinically suspected to be affected based on ultrasound findings. In principle, the approach presented by Zhang et al. [99] would be technically feasible for NIPS of low-risk pregnancies at much earlier (~10 weeks') gestations. However, further technical refinements and demonstration of cost-effectiveness will be required before entering clinical practice.

Mouse Models of Apert Syndrome

Although valuable insights into the pathogenesis of Apert syndrome have been gained from the study of affected fetuses (reviewed by [88]; see also Chap. 5), the use of genetically equivalent mouse models enables substantially more detailed studies of the pathogenesis of malformation. For example, the use of one such model, the *Fgfr2*$^{\Delta IIIc/+}$ mouse, to investigate the pathogenic mechanism of *FGFR2*-exon IIIc deletions was discussed in Section "Beyond the canonical mutations: rare molecular causes of Apert syndrome." Regarding the canonical mutations, an initial barrier to creating mouse models was that heterozygous Apert syndrome mice are more severely affected in their craniofacial development than humans with the equivalent mutations, making it effectively impossible to breed Apert syndrome mouse lines directly. Rather, the mice must be created by first making lines in which the Apert syndrome mutation is present but not expressed at a high level, and then secondarily uncovering the functioning mutation by further genetic manipulation. Using such targeting strategies, the first model of the p.Ser252Trp mutation was made by Chen et al. [9] and the first model of the Pro253Arg was made by Yin et al. [95] (conveniently, the cDNA numbering of human *FGFR2* and orthologous mouse *Fgfr2* genes is identical; with the aim to distinguish more clearly the outcome of work performed on mice and humans, the canonical mutations in mice are denoted S252W and P253R for the remainder of this chapter). Independently generated S252W and P253R models were also subsequently made [86, 87]. These mice have been used to study the developmental origins of the morphological abnormalities that occur in Apert syndrome (summarized in Table 4.4; see [23], for review), and are particularly valuable for studies that address pathways of perturbed FGFR2 signaling in malformation and how these may be therapeutically manipulated (Section "Pathways activated in Apert syndrome and approaches to therapeutic inhibition").

One striking observation from the examination of these Apert syndrome mice is that although they reliably manifest craniosynostosis (Table 4.4), only very rarely do they exhibit digital syndactyly, so that the development of this latter phenotype cannot be fully investigated. More usefully, the coronal sutures are nearly always fused at birth in Apert syndrome model mice, whereas the sagittal suture starts off as patent but with a prominent cartilaginous element. Detailed analysis of the coronal suture [25] found that in E13.5 *Fgfr2*$^{S252W/+}$ mutant mice, the osteogenic fronts of the newly appearing basal coronal sutures are already in a state of incipient fusion. In the mid/upper coronal sutures, the anlage of the frontal and parietal bones is also substantially closer in mutant than wild-type animals, with complete fusion in the mutants by birth (postnatal day [P]0) (Fig. 4.8a). A systematic analysis of markers of proliferation, differentiation, and apoptosis concluded that the primary cause of craniosynostosis in *Fgfr2*$^{S252W/+}$ mice is early (embryonic day [E]12) loss of basal sutural mesenchyme. This represents a differentiation defect involving the osteogenic fronts expressing activated Fgfr2, leading these fronts to unite to form a contiguous skeletogenic membrane. As development proceeds, the superior part of the coronal suture initially forms in mutants, but fuses as a

Table 4.4 Survey of major anatomical features observed in engineered Apert syndrome mouse mutants

	Design	Cranial sutures	Cranial base	Facial	Other organs	Skeleton	Stature	Survival	Fertility	References
S252W	Intronic loxP-*neo* cassette upstream of exon IIIa inhibits expression	Coronal synostosis from E18.5; calvarial bones 25% thinner; primary differentiation defect of sutures; secondary increase in apoptosis; normal proliferation	Normal synchondroses of presphenoid-sphenoidal, basisphenoid-occipital, and basioccipital-exoccipital bones; short presphenoid bone	Midface hypoplasia; malocclusion		Shortened hindlimbs, reduced bone density, sparse trabecular network, and delayed secondary ossification centers in tibial epiphyses; no limb syndactyly	<80% wild-type	Ranging from death at 20 day in severely runted mice to survival to adulthood	Female, infertile; male, much reduced (1 fertile male obtained)	Chen et al. [9, 10], Holmes et al. [25]
S252W	Intronic loxP-*neo* cassette downstream of exon IIIa inhibits expression	Coronal and lambdoid synostosis from E18.5; ectopic cartilage in sagittal suture E16.5–E18.5 and synostosis from P1; widened interfrontal (metopic) suture	Increased cartilage of basicranium	Thickened nasal cartilage	Complete cartilage sleeve of the trachea	No limb syndactyly; fusion of sternal bones; disorganized growth plates of long bones	Birthweight 83% of wild-type	Death at 24–36 h postnatally (respiratory), except with incomplete *neo* excision	Insufficient survival to test	Wang et al. [86]

P253R	Intronic loxP-*neo* cassette upstream of exon IIIa inhibits expression	Coronal synostosis; delayed fusion of posterior frontal suture (cartilage absent compared to controls); ectopic cartilage in sagittal suture	Retardation of cranial base synchondroses	Reduced nasale–nasion distance		Syndactyly present in 3/40 individuals; delayed ossification centers in tibial epiphysis	Birthweight 90% of wild-type; weight 50–60% of controls at 3 weeks	35% death by P20; 45% by 6 months; 20% survived to adulthood	Normal	Yin et al. [95]
P253R	Intronic loxP-*neo* cassette downstream of exon IIIa inhibits expression	Coronal synostosis at P0; increased osteoid in sagittal and lambdoid sutures; ectopic cartilage in sagittal suture	Shortened anterior cranial base	10% reduction of maxilla and nasal region; bilateral incomplete fusion of primary and secondary palatal shelves		Abnormal sternal fusions; no syndactyly	Normal birthweight; 40% reduction in weight by P5	40% death at 24–36 h; 1/20 survived to P14	Insufficient survival to test	Wang et al. [87]
ΔIIIc	Complete deletion of exon IIIc	Coronal synostosis at E18		Truncated maxilla; fused zygomatic arch bones	Abnormal lung lobulation; incomplete alveolarization; small kidneys	Precocious ossification of the intersternebral cartilage; no syndactyly	Mild reduction in birthweight in 90%; severe in 10%	100% death by P9	No survival	Hajihosseini et al. [21]

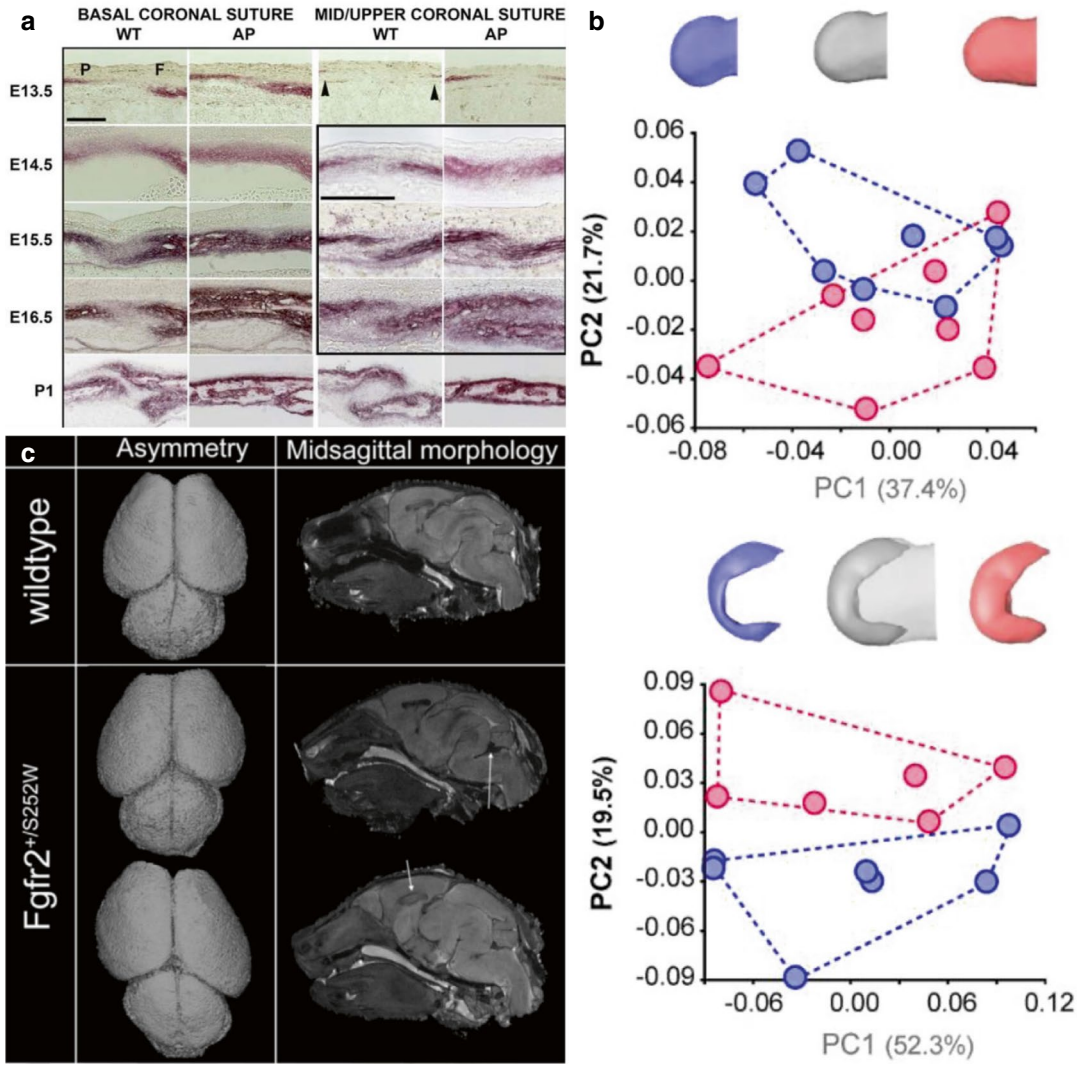

Fig. 4.8 Abnormal developmental phenotypes in Apert syndrome mutant mouse models. (**a**) Coronal suture. Sagittal cross-sections of alkaline phosphatase-stained sutures at two levels (left, basal; right, mid/upper) in wild-type (WT) and *Fgfr2*$^{S252W/+}$ mutant (AP) mice, from E13.5 (top) to postnatal day 1 (P1, bottom). At E13.5, abnormality of the basal suture is already evident, with only a narrow gap in the alkaline phosphatase-stained territories, which have merged 1 day later. At higher levels the coronal suture is initially patent but evidently narrower than in WT, and has closed by P1. Note that the growing parietal bone tip overlaps the frontal bone tip in the normal coronal suture. Scale bars are 100 μm (reproduced from: [25]). (**b**) Limb bud morphology in E11 WT (blue) and Apert syndrome mutant *Fgfr2*$^{P253R/+}$ (red) mice, using optical projection tomography fluorescence scanning to analyze shape (upper panel) and whole-mount in situ hybridization/transmission scanning to analyze expression of *Dusp6*, a direct target of Fgfr2-mediated signaling (lower panel: renditions of limb buds are not shown at the same scale). Gray images represent regions of similarity between the two genotypes. The lower plots in each panel show principal component analyses, indicating that the two genotypes are largely separable at this embryonic stage, particularly based on *Dusp6* expression, which is more extensive in the mutant limb buds that exhibit a narrower but longer shape profile (reproduced from: [50]). (**c**) Brains from P0 mice analyzed by magnetic resonance microscopy. Compared to wild-type, the Apert syndrome *Fgfr2*$^{S252W/+}$ mutant mouse brains more frequently showed asymmetry (two examples at mid/lower left), enlarged fourth ventricle (white arrow in middle right image), and arched corpus callosum (white arrow in bottom right image). (Reproduced from: [2])

result of localized induction of osteogenesis within the narrow margin of mesenchyme separating the adjacent osteogenic fronts [25]. Using a Mesp1-cre driver it was shown that expression of the Apert syndrome mutation in cephalic mesoderm (which includes the mesodermally derived coronal suture) was sufficient to cause coronal suture fusion [24].

Following on from this work, a series of detailed descriptive studies has been published addressing various elements of Apert syndrome mouse morphology, including several aspects of facial and mandibular growth [26, 28, 48, 56] as well as palate development [49]; the interested reader should consult the original articles for further details. Subtle abnormalities of the limbs, including forefoot bones, have been documented using advanced imaging techniques and have been associated with increased expression in *Fgfr2*$^{P253R/+}$ mutants of the target gene *Dusp6*; this first occurred at E10.5, ~12 h before any morphological abnormality (a slightly smaller and dorsoventrally thicker limb paddle in mutant; Fig. 4.7b) became evident [50]. However, as noted above, these early limb bud abnormalities, although consistently present, do not result in syndactyly later in development. Also of particular interest, study of the brain using magnetic resonance microscopy has shown that both Apert syndrome mouse mutants exhibit variable but significant primary abnormalities of brain morphology, for example severe brain asymmetry, arched corpus callosum, and/or fourth ventricle enlargement [2] (Fig. 4.7c). These observations mirror clinical observations of the brain in Apert syndrome and are relevant to the question whether these represent primary neurological abnormalities or are secondary to cranial suture fusion (see Chap. 5).

Pathways Activated in Apert Syndrome and Approaches to Therapeutic Inhibition

As discussed in Section "Biological and pathological context: FGFR2 structure, function, and comparative mutation patterns in Apert, Crouzon and Pfeiffer syndromes" and illustrated in Fig. 4.2, FGFR-mediated signal activation may occur through multiple different pathways according to the cellular and developmental context. This raises the question, "what are the most important signaling pathways perturbed by Apert syndrome mutations?" I will start by presenting a beautiful experiment that helps to address this question.

Analysis of Mouse Models

Using a previously constructed mouse model of the S252W mutation [9] (see previous section), Shukla et al. [81] experimented with two distinct methods to prevent the developmental abnormalities caused by the mutation. One approach used a short hairpin RNA (shRNA) to target the specific Apert syndrome mutant allele. Owing to different codon usage between human and mouse, the substitution required in the mouse to encode S252W is not TCG > TGG (human), but TCA > TGG (substituted bases underlined). This means that there is a dinucleotide difference in the mouse between the normal and Apert syndrome mutant sequence, making direct shRNA-based targeting somewhat more specific. After generating a transgenic mouse containing a specific U6shRNA construct, the authors crossed this to yield mice doubly heterozygous with the Apert syndrome mutation. Remarkably, these mice had normal craniofacial phenotypes [81]. Importantly, comparison of both lung and thymic tissues showed prominently increased phospho-ERK (extracellular signal-related kinase; pERK) in the Apert syndrome mutants, which normalized when the shRNA transgene was additionally present. Phosphorylation of ERK (which is encoded by the genes *MAPK1* and *MAPK3*) is the final step in the activation of the important RAS–MEK–ERK (also referred to as the RAS–MAPK or p42/44) signaling pathway (Fig. 4.9a) [39]. Therefore, this result was consistent with, but did not prove, that craniosynostosis and other malformations resulted from activation of this pathway.

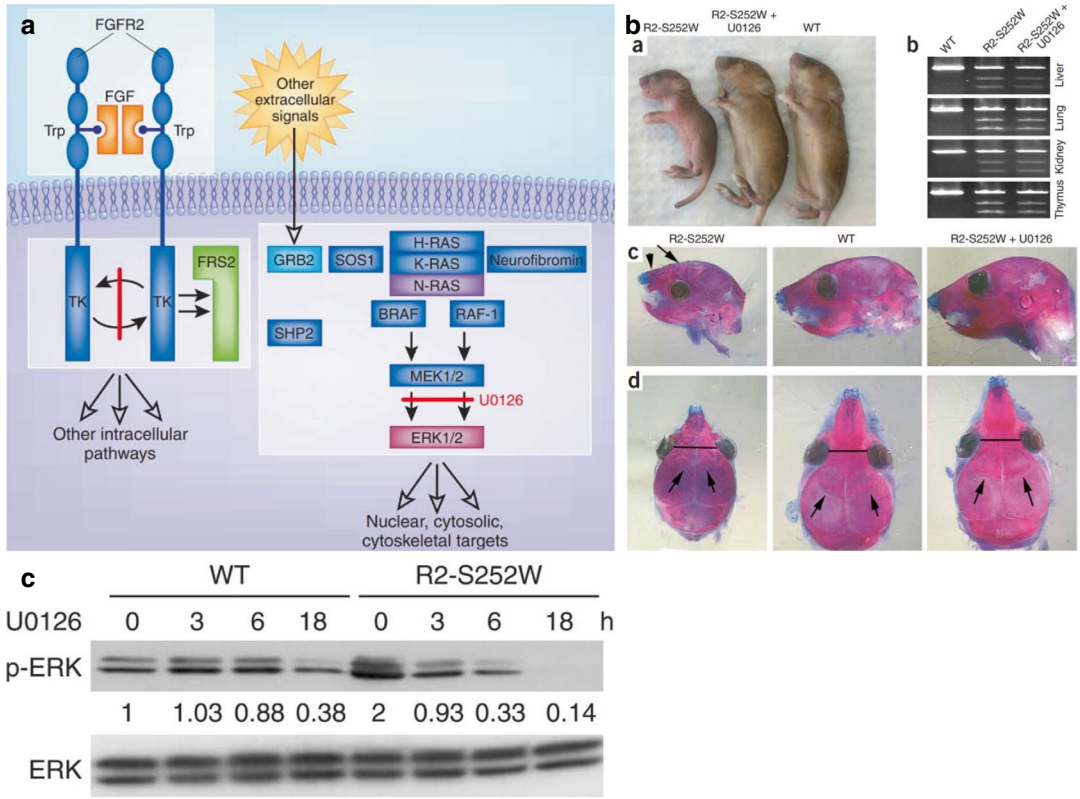

Fig. 4.9 Correction of morphological abnormalities in Apert syndrome mouse using a MEK1/2 inhibitor. (**a**) Schematic of signaling from mutant FGFR2 molecules through the RAS–MAPK pathway. The position of U0126 blockade of MEK1/2 is indicated by the red bar (figure adapted from: [89]). (**b**) Mouse phenotypes and mutation confirmation. Panels a, c, and d show the whole body (a) and cleared Alizarin red/Alcian blue-stained skull (c,d), all at P8, in mice heterozygous for the S252W mutation (R2-S252W) that were either untreated or treated with U0126, and in genotypically normal wild-type controls (WT). Panel b shows a cDNA-based assay for *FGFR2* expression; the pair of lower bands are diagnostic for presence of the engineered mutation. (**c**) Immunoblot measurement of phosphorylation of the downstream effector proteins ERK1/2 in wild-type mice (WT, left) and S252W-mutant mice (right). Note how the total amount of ERK remains unchanged with U0126 treatment (lower panel), but the active phospho-ERK (p-ERK) transitions from a hyperactivated state (time zero) to complete loss (inactivation) by 18 h. (Figure parts b, c from: [81])

To test this possibility directly, Shukla and colleagues [81] injected pregnant female mice bearing embryos heterozygous for the S252W mutation with a chemical, U0126, originally designed as an anti-cancer drug via selective inhibition of MEK1/2, a critical intermediate component of the RAS–MAPK pathway (Fig. 4.9a). The injections started at E13 of gestation, then continued in the postnatal period up to P26. Remarkably, the treated mice were born without craniosynostosis and, unlike genetically identical but untreated pups, several grew up to be fertile (Fig. 4.9b). Tissue analysis confirmed that the U0126 treatment not only corrected the excessive ERK phosphorylation present in mutant mice, but after 18 h it was abolished altogether; in other words, it was overcorrected (Fig. 4.9c). Similar conclusions were obtained for the P253R mouse model, this time using treatments with a different MEK1/2 inhibitor (PD98059), conducted on in vitro cultured calvaria and femur explants [95].

These groundbreaking experiments using pharmacological inhibition convincingly demon-

strated that several of the major malformative features of Apert syndrome arise through hyperactivation of the RAS–MAPK signaling pathway, consistent with other genetic data that this pathway is especially important in FGF receptor signal transduction [8]. Moreover, they illustrate a powerful proof-of-principle that Apert syndrome-associated malformations are in theory correctable, if therapy could be introduced early enough during the pregnancy. However, this work also highlights the major challenges of contemplating such an approach. In pregnancy, except in the rare cases at high risk (when one of the parents is affected with the condition), Apert syndrome is only routinely detected (if at all) by the ultrasound-based identification of anatomical abnormality; by definition, this would be too late to start preventative therapy. Another aspect is the potential for intrauterine therapies to cause harm; U0126 was never licensed for clinical use owing to toxicity, and Fig. 4.9c illustrates that overdosing could readily abolish the normal physiological functions of ERK activation. The possibility remains that inhibitory therapies based on the principles illustrated above might be used for secondary prevention of progression following surgery; however, this particular application does not seem to have advanced greatly since the original report by Shukla et al. [81].

Importantly, ERK1/2 activation does not mediate all Apert syndrome-related pathology. Analysis of previously described mouse models (Table 4.4) also demonstrated increased phosphorylation (hence activation) of the p38 serine threonine kinase signaling pathway, mediated by a family of MAPKs (encoded by the genes *MAPK11*, *−12*, *−13* and *−14*) that are activated by cellular stress and/or several growth factors and cytokines [10, 39, 87]. Chen et al. [10] focused on development of the long bones and vertebrae in S252W mice, observing reduced bone density, sparser trabecular network, and delayed secondary ossification centers in the tibial epiphyses of mutants (Table 4.4); this was associated with reduced markers of proliferation and differentiation in mutant tibial growth plates and cells. (These investigators attempted to counter any non-specific effects from malnutrition owing to dental malocclusion in mutants by cutting the overgrown incisor teeth.) In cultured mesenchymal stem cells (MSCs), increased phosphorylation of both pERK1/2 and p38 was observed. Treatment of cultured tibiae with specific inhibitors for the two pathways (PD98059 and SB203580, respectively) showed greater restoration of phenotype using the latter inhibitor, suggesting a greater influence of p38 MAPK function [10]. Excessive osteoclast activation has also been implicated in the abnormal long bone phenotype of Apert syndrome mutants [80].

Downstream from RAS–MAPK signaling, the master osteogenic regulator RUNX2 has been identified as a further potential therapeutic target. Intraperitoneal injection of pregnant female mice with juglone, an inhibitor of PIN1 (peptidyl-prolyl cis–trans isomerase NIMA-interacting 1), prevented the development of craniosynostosis in *Fgfr2*$^{S252W/+}$ mutant offspring. This effect is believed to be mediated through destabilization of RUNX2, antagonizing stabilizing RUNX2 post-translational modifications induced by the activating *Fgfr2*$^{S252W/+}$ mutation [35, 79, 97]. However, given that PIN1 has many other biological targets, use of juglone therapeutically would raise safety concerns analogous to those applying to MEK1 inhibitors. Evidence for activation of the canonical Wnt (wingless-type MMTV integration site family)/β-catenin signaling pathway in the cranial sutures has also been presented [51]. How the FGF and WNT signaling pathways interlink requires further elucidation.

Recent Therapeutic Approaches

In summary, the above studies illustrate the complexity of pharmacological inhibition of signaling downstream of FGFR2 activation, which has led to more targeted approaches. For example, crossing of *Fgfr2*$^{S252W/+}$ mice with a transgenic mouse expressing a soluble (extracellular) portion of the Fgfr2^{S252W} mutant receptor showed modest amelioration of the craniofacial phenotype, attributed to reduction of FGFR2 signaling by acting as a competitive decoy receptor [55]. However, it would be challenging to exploit this

approach as a therapeutic owing to likely non-specific effects on other aspects of FGFR-mediated signaling. A more promising strategy, encouraged by the success of the transgenic shRNA experiment described above [81], has been to explore different methods to deliver either an shRNA or short interfering RNA (siRNA) targeting one of the canonical mutations, to achieve specific knockdown of mutant FGFR2. For example, by linking an shRNA construct to AAV9 (adeno-associated virus 9), followed by calvarial injection of virus particles at P0 and P4, reduced expression of the mutant *Fgfr2* mRNA and modest rescue of the suture fusion phenotype of the $Fgfr2^{P253R/+}$ Apert syndrome mouse was achieved [43]. However, systemic delivery would be preferable for wider therapeutic benefit. An exosome-based delivery of siRNA targeting $Fgfr2^{S252W/+}$ tissue has also been explored, but to date only in vitro, by incubation of loaded exosomes with primary calvarial osteoblast-like cells [57].

Concluding Comments

Most of this chapter has been taken up by exploring the pathological consequences of the two canonical Apert syndrome-causing mutations that arise in the *FGFR2* gene. It is hard for the human brain to conceptualize what a tiny proportion of the human genome this represents; a smaller proportion, for example, than the lives elapsed of anyone reading this chapter in relation to the age of the known universe. Although the amount, and detail, that we have learnt about these two canonical mutations over the past three decades is remarkable, this must be tempered with a strong measure of humility, because the information has so far had a rather limited impact on the lives of those affected by Apert syndrome. However, on a positive note, the basic scientific knowledge presented here, combined with ongoing and rapid technological advances, provides optimism that new approaches to both prevention (Section "Clinical Implications of Selfish Spermatogonial Selection") and therapy (Section "Recent Therapeutic Approaches") will emerge before another three decades pass.

Acknowledgments I thank my brilliant colleagues Elena Bochukova, Dominique Davidson, Aimee Fenwick, Anne Goriely, Ruth Hansen, John Heath, Shih-hsin Kan, Jasmine Lim, Geoffrey Maher, Gil McVean, Gillian Morriss-Kay, Michael Oldridge, Susannah Patey, Sarah Smithson and Steve Twigg, who accompanied me during my personal journey of discovery into Apert syndrome and made key contributions to the work presented here. The Wellcome Trust provided the majority of the funding for my laboratory. This chapter is dedicated to the memory of my mentor, Sir David Weatherall FRS, whose steadfast support enabled this research to happen.

References

1. Ahmed Z, Schuller AC, Suhling K, Tregidgo C, Ladbury JE. Extracellular point mutations in FGFR2 elicit unexpected changes in intracellular signalling. Biochem J. 2008;413(1):37–49.
2. Aldridge K, Hill CA, Austin JR, Percival C, Martinez-Abadias N, Neuberger T, Wang Y, Jabs EW, Richtsmeier JT. Brain phenotypes in two FGFR2 mouse models for Apert syndrome. Dev Dyn. 2010;239(3):987–97.
3. Allanson JE. Germinal mosaicism in Apert syndrome. Clin Genet. 1986;29(5):429–33.
4. Anderson J, Burns HD, Enriquez-Harris P, Wilkie AOM, Heath JK. Apert syndrome mutations in fibroblast growth factor receptor 2 exhibit increased affinity for FGF ligand. Hum Mol Genet. 1998;7(9):1475–83.
5. Bergeron LA, Besenbacher S, Turner T, Versoza CJ, Wang RJ, Price AL, Armstrong E, Riera M, Carlson J, Chen HY, Hahn MW, Harris K, Kleppe AS, Lopez-Nandam EH, Moorjani P, Pfeifer SP, Tiley GP, Yoder AD, Zhang G, Schierup MH. The Mutationathon highlights the importance of reaching standardization in estimates of pedigree-based germline mutation rates. eLife. 2022;11:e73577.
6. Blank CE. Apert's syndrome (a type of acrocephalosyndactyly)-observations on a British series of thirty-nine cases. Ann Hum Genet. 1960;24:151–64.
7. Bochukova EG, Roscioli T, Hedges DJ, Taylor IB, Johnson D, David DJ, Deininger PL, Wilkie AOM. Rare mutations of *FGFR2* causing Apert syndrome: identification of the first partial gene deletion, and an *Alu* element insertion from a new subfamily. Hum Mutat. 2009;30(2):204–11.
8. Brewer JR, Mazot P, Soriano P. Genetic insights into the mechanisms of Fgf signaling. Genes Dev. 2016;30(7):751–71.
9. Chen L, Li D, Li C, Engel A, Deng CX. A Ser252Trp [corrected] substitution in mouse fibroblast growth

factor receptor 2 (Fgfr2) results in craniosynostosis. Bone. 2003;33(2):169–78.
10. Chen P, Zhang L, Weng T, Zhang S, Sun S, Chang M, Li Y, Zhang B, Zhang L. A Ser252Trp mutation in fibroblast growth factor receptor 2 (FGFR2) mimicking human Apert syndrome reveals an essential role for FGF signaling in the regulation of endochondral bone formation. PLoS One. 2014;9(1):e87311.
11. Choi SK, Yoon SR, Calabrese P, Arnheim N. A germline-selective advantage rather than an increased mutation rate can explain some unexpectedly common human disease mutations. Proc Natl Acad Sci USA. 2008;105(29):10143–8.
12. Chun K, Teebi AS, Azimi C, Steele L, Ray PN. Screening of patients with craniosynostosis: molecular strategy. Am J Med Genet A. 2003;120A(4):470–3.
13. Farmer DT, Mlcochova H, Zhou Y, Koelling N, Wang G, Ashley N, Bugacov H, Chen HJ, Parvez R, Tseng KC, Merrill AE, Maxson RE Jr, Wilkie AOM, Crump JG, Twigg SRF. The developing mouse coronal suture at single-cell resolution. Nat Commun. 2021;12(1):4797.
14. Fearon JA, Podner C. Apert syndrome: evaluation of a treatment algorithm. Plast Reconstr Surg. 2013;131(1):132–42.
15. Fenwick AL, Bowdin SC, Klatt RE, Wilkie AOM. A deletion of *FGFR2* creating a chimeric IIIb/IIIc exon in a child with Apert syndrome. BMC Med Genet. 2011;12:122.
16. Goetz R, Mohammadi M. Exploring mechanisms of FGF signalling through the lens of structural biology. Nat Rev Mol Cell Biol. 2013;14(3):166–80.
17. Goriely A, Wilkie AOM. Paternal age effect mutations and selfish spermatogonial selection: causes and consequences for human disease. Am J Hum Genet. 2012;90(2):175–200.
18. Goriely A, McVean GA, Rojmyr M, Ingemarsson B, Wilkie AOM. Evidence for selective advantage of pathogenic FGFR2 mutations in the male germ line. Science. 2003;301(5633):643–6.
19. Goriely A, McVean GA, van Pelt AM, O'Rourke AW, Wall SA, de Rooij DG, Wilkie AOM. Gain-of-function amino acid substitutions drive positive selection of *FGFR2* mutations in human spermatogonia. Proc Natl Acad Sci USA. 2005;102(17):6051–6.
20. Goriely A, Lord H, Lim J, Johnson D, Lester T, Firth HV, Wilkie AOM. Germline and somatic mosaicism for *FGFR2* mutation in the mother of a child with Crouzon syndrome: Implications for genetic testing in "paternal age-effect" syndromes. Am J Med Genet A. 2010;152A(8):2067–73.
21. Hajihosseini MK, Wilson S, De Moerlooze L, Dickson C. A splicing switch and gain-of-function mutation in *FgfR2-IIIc* hemizygotes causes Apert/Pfeiffer-syndrome-like phenotypes. Proc Natl Acad Sci USA. 2001;98(7):3855–60.
22. Hajihosseini MK, Duarte R, Pegrum J, Donjacour A, Lana-Elola E, Rice DP, Sharpe J, Dickson C. Evidence that Fgf10 contributes to the skeletal and visceral defects of an Apert syndrome mouse model. Dev Dyn. 2009;238(2):376–85.
23. Holmes G. Mouse models of Apert syndrome. Childs Nerv Syst. 2012;28(9):1505–10.
24. Holmes G, Basilico C. Mesodermal expression of $Fgfr2^{S252W}$ is necessary and sufficient to induce craniosynostosis in a mouse model of Apert syndrome. Dev Biol. 2012;368(2):283–93.
25. Holmes G, Rothschild G, Roy UB, Deng CX, Mansukhani A, Basilico C. Early onset of craniosynostosis in an Apert mouse model reveals critical features of this pathology. Dev Biol. 2009;328(2):273–84.
26. Holmes G, O'Rourke C, Motch Perrine SM, Lu N, van Bakel H, Richtsmeier JT, Jabs EW. Midface and upper airway dysgenesis in FGFR2-related craniosynostosis involves multiple tissue-specific and cell cycle effects. Development. 2018;145(19):dev166488.
27. Holmes G, Gonzalez-Reiche AS, Saturne M, Motch Perrine SM, Zhou X, Borges AC, Shewale B, Richtsmeier JT, Zhang B, van Bakel H, Jabs EW. Single-cell analysis identifies a key role for *Hhip* in murine coronal suture development. Nat Commun. 2021;12(1):7132.
28. Hoshino Y, Takechi M, Moazen M, Steacy M, Koyabu D, Furutera T, Ninomiya Y, Nuri T, Pauws E, Iseki S. Synchondrosis fusion contributes to the progression of postnatal craniofacial dysmorphology in syndromic craniosynostosis. J Anat. 2023;242(3):387–401.
29. Ibrahimi OA, Eliseenkova AV, Plotnikov AN, Yu K, Ornitz DM, Mohammadi M. Structural basis for fibroblast growth factor receptor 2 activation in Apert syndrome. Proc Natl Acad Sci USA. 2001;98(13):7182–7.
30. Ibrahimi OA, Zhang F, Eliseenkova AV, Itoh N, Linhardt RJ, Mohammadi M. Biochemical analysis of pathogenic ligand-dependent FGFR2 mutations suggests distinct pathophysiological mechanisms for craniofacial and limb abnormalities. Hum Mol Genet. 2004;13(19):2313–24.
31. Jabs EW, Muller U, Li X, Ma L, Luo W, Haworth IS, Klisak I, Sparkes R, Warman ML, Mulliken JB, et al. A mutation in the homeodomain of the human MSX2 gene in a family affected with autosomal dominant craniosynostosis. Cell. 1993;75(3):443–50.
32. Jabs EW, Li X, Scott AF, Meyers G, Chen W, Eccles M, Mao JI, Charnas LR, Jackson CE, Jaye M. Jackson-Weiss and Crouzon syndromes are allelic with mutations in fibroblast growth factor receptor 2. Nat Genet. 1994;8(3):275–9.
33. Kan S-h, Elanko N, Johnson D, Cornejo-Roldan L, Cook J, Reich EW, Tomkins S, Verloes A, Twigg SRF, Rannan-Eliya S, McDonald-McGinn DM, Zackai EH, Wall SA, Muenke M, Wilkie AOM. Genomic screening of fibroblast growth factor receptor 2 reveals a wide spectrum of mutations in patients with syndromic craniosynostosis. Am J Hum Genet. 2002;70(2):472–86.
34. Karczewski KJ, Francioli LC, Tiao G, Cummings BB, Alfoldi J, Wang Q, Collins RL, Laricchia KM, Ganna A, Birnbaum DP, Gauthier LD, Brand H,

Solomonson M, Watts NA, Rhodes D, Singer-Berk M, England EM, Seaby EG, Kosmicki JA, Walters RK, Tashman K, Farjoun Y, Banks E, Poterba T, Wang A, Seed C, Whiffin N, Chong JX, Samocha KE, Pierce-Hoffman E, Zappala Z, O'Donnell-Luria AH, Minikel EV, Weisburd B, Lek M, Ware JS, Vittal C, Armean IM, Bergelson L, Cibulskis K, Connolly KM, Covarrubias M, Donnelly S, Ferriera S, Gabriel S, Gentry J, Gupta N, Jeandet T, Kaplan D, Llanwarne C, Munshi R, Novod S, Petrillo N, Roazen D, Ruano-Rubio V, Saltzman A, Schleicher M, Soto J, Tibbetts K, Tolonen C, Wade G, Talkowski ME, C. Genome Aggregation Database, Neale BM, Daly MJ, MacArthur DG. The mutational constraint spectrum quantified from variation in 141,456 humans. Nature. 2020;581(7809):434–43.

35. Kim B, Shin H, Kim W, Kim H, Cho Y, Yoon H, Baek J, Woo K, Lee Y, Ryoo H. PIN1 attenuation improves midface hypoplasia in a mouse model of Apert syndrome. J Dent Res. 2020;99(2):223–32.
36. Kitadate Y, Jorg DJ, Tokue M, Maruyama A, Ichikawa R, Tsuchiya S, Segi-Nishida E, Nakagawa T, Uchida A, Kimura-Yoshida C, Mizuno S, Sugiyama F, Azami T, Ema M, Noda C, Kobayashi S, Matsuo I, Kanai Y, Nagasawa T, Sugimoto Y, Takahashi S, Simons BD, Yoshida S. Competition for mitogens regulates spermatogenic stem cell homeostasis in an open niche. Cell Stem Cell. 2019;24(1):79–92 e76.
37. Lajeunie E, Ma HW, Bonaventure J, Munnich A, Le Merrer M, Renier D. *FGFR2* mutations in Pfeiffer syndrome. Nat Genet. 1995;9(2):108.
38. Lajeunie E, Cameron R, El Ghouzzi V, de Parseval N, Journeau P, Gonzales M, Delezoide AL, Bonaventure J, Le Merrer M, Renier D. Clinical variability in patients with Apert's syndrome. J Neurosurg. 1999;90(3):443–7.
39. Lavoie H, Gagnon J, Therrien M. ERK signalling: a master regulator of cell behaviour, life and fate. Nat Rev Mol Cell Biol. 2020;21(10):607–32.
40. Lim J, Maher GJ, Turner GD, Dudka-Ruszkowska W, Taylor S, Rajpert-De Meyts E, Goriely A, Wilkie AOM. Selfish spermatogonial selection: evidence from an immunohistochemical screen in testes of elderly men. PLoS One. 2012;7(8):e42382.
41. Liu Z, Xu J, Colvin JS, Ornitz DM. Coordination of chondrogenesis and osteogenesis by fibroblast growth factor 18. Genes Dev. 2002;16(7):859–69.
42. Lumaka A, Mubungu G, Mukaba P, Mutantu P, Luyeye G, Corveleyn A, Tady BP, Lukusa Tshilobo P, Devriendt K. A novel heterozygous mutation of three consecutive nucleotides causing Apert syndrome in a Congolese family. Eur J Med Genet. 2014;57(4):169–73.
43. Luo F, Xie Y, Wang Z, Huang J, Tan Q, Sun X, Li F, Li C, Liu M, Zhang D, Xu M, Su N, Ni Z, Jiang W, Chang J, Chen H, Chen S, Xu X, Deng C, Wang Z, Du X, Chen L. Adeno-associated virus-mediated RNAi against mutant alleles attenuates abnormal calvarial phenotypes in an apert syndrome mouse model. Mol Ther Nucleic Acids. 2018;13:291–302.
44. Maher GJ, Goriely A, Wilkie AOM. Cellular evidence for selfish spermatogonial selection in aged human testes. Andrology. 2014;2(3):304–14.
45. Maher GJ, McGowan SJ, Giannoulatou E, Verrill C, Goriely A, Wilkie AOM. Visualizing the origins of selfish de novo mutations in individual seminiferous tubules of human testes. Proc Natl Acad Sci USA. 2016;113(9):2454–9.
46. Maher GJ, Ralph HK, Ding Z, Koelling N, Mlcochova H, Giannoulatou E, Dhami P, Paul DS, Stricker SH, Beck S, McVean G, Wilkie AOM, Goriely A. Selfish mutations dysregulating RAS-MAPK signaling are pervasive in aged human testes. Genome Res. 2018;28(12):1779–90.
47. Martin LA, Assif N, Gilbert M, Wijewarnasuriya D, Seandel M. Enhanced fitness of adult spermatogonial stem cells bearing a paternal age-associated FGFR2 mutation. Stem Cell Rep. 2014;3(2):219–26.
48. Martinez-Abadias N, Percival C, Aldridge K, Hill CA, Ryan T, Sirivunnabood S, Wang Y, Jabs EW, Richtsmeier JT. Beyond the closed suture in Apert syndrome mouse models: evidence of primary effects of FGFR2 signaling on facial shape at birth. Dev Dyn. 2010;239(11):3058–71.
49. Martinez-Abadias N, Holmes G, Pankratz T, Wang Y, Zhou X, Jabs EW, Richtsmeier JT. From shape to cells: mouse models reveal mechanisms altering palate development in Apert syndrome. Dis Model Mech. 2013;6(3):768–79.
50. Martinez-Abadias N, Mateu Estivill R, Sastre Tomas J, Motch Perrine S, Yoon M, Robert-Moreno A, Swoger J, Russo L, Kawasaki K, Richtsmeier J, Sharpe J. Quantification of gene expression patterns to reveal the origins of abnormal morphogenesis. elife. 2018;7:e36405.
51. Min Swe NM, Kobayashi Y, Kamimoto H, Moriyama K. Aberrantly activated Wnt/beta-catenin pathway co-receptors LRP5 and LRP6 regulate osteoblast differentiation in the developing coronal sutures of an Apert syndrome (*Fgfr2*$^{S252W/+}$) mouse model. Dev Dyn. 2021;250(3):465–76.
52. Mohammadi M, Olsen SK, Ibrahimi OA. Structural basis for fibroblast growth factor receptor activation. Cytokine Growth Factor Rev. 2005;16(2):107–37.
53. Moloney DM, Slaney SF, Oldridge M, Wall SA, Sahlin P, Stenman G, Wilkie AOM. Exclusive paternal origin of new mutations in Apert syndrome. Nat Genet. 1996;13(1):48–53.
54. Monaco AP, Neve RL, Colletti-Feener C, Bertelson CJ, Kurnit DM, Kunkel LM. Isolation of candidate cDNAs for portions of the Duchenne muscular dystrophy gene. Nature. 1986;323(6089):646–50.
55. Morita J, Nakamura M, Kobayashi Y, Deng CX, Funato N, Moriyama K. Soluble form of FGFR2 with S252W partially prevents craniosynostosis of the Apert mouse model. Dev Dyn. 2014;243(4):560–7.
56. Motch Perrine SM, Wu M, Stephens NB, Kriti D, van Bakel H, Jabs EW, Richtsmeier JT. Mandibular dysmorphology due to abnormal embryonic osteogenesis

in FGFR2-related craniosynostosis mice. Dis Model Mech. 2019;12(5)
57. Myo AC, Kobayashi Y, Niki Y, Kamimoto H, Moriyama K. Exosome-mediated small interfering RNA delivery inhibits aberrant osteoblast differentiation in Apert syndrome model mice. Arch Oral Biol. 2023;153:105753.
58. Ohbayashi N, Shibayama M, Kurotaki Y, Imanishi M, Fujimori T, Itoh N, Takada S. FGF18 is required for normal cell proliferation and differentiation during osteogenesis and chondrogenesis. Genes Dev. 2002;16(7):870–9.
59. Ohishi A, Nishimura G, Kato F, Ono H, Maruwaka K, Ago M, Suzumura H, Hirose E, Uchida Y, Fukami M, Ogata T. Mutation analysis of *FGFR1-3* in 11 Japanese patients with syndromic craniosynostoses. Am J Med Genet A. 2017;173(1):157–62.
60. Oldridge M, Lunt PW, Zackai EH, McDonald-McGinn DM, Muenke M, Moloney DM, Twigg SR, Heath JK, Howard TD, Hoganson G, Gagnon DM, Jabs EW, Wilkie AOM. Genotype-phenotype correlation for nucleotide substitutions in the IgII-IgIII linker of *FGFR2*. Hum Mol Genet. 1997;6(1):137–43.
61. Oldridge M, Zackai EH, McDonald-McGinn DM, Iseki S, Morriss-Kay GM, Twigg SR, Johnson D, Wall SA, Jiang W, Theda C, Jabs EW, Wilkie AOM. *De novo Alu*-element insertions in *FGFR2* identify a distinct pathological basis for Apert syndrome. Am J Hum Genet. 1999;64(2):446–61.
62. Ornitz DM, Itoh N. The Fibroblast Growth Factor signaling pathway. Wiley Interdiscip Rev Dev Biol. 2015;4(3):215–66.
63. Park WJ, Theda C, Maestri NE, Meyers GA, Fryburg JS, Dufresne C, Cohen MM Jr, Jabs EW. Analysis of phenotypic features and FGFR2 mutations in Apert syndrome. Am J Hum Genet. 1995;57(2):321–8.
64. Passos-Bueno MR, Sertie AL, Zatz M, Richieri-Costa A. Pfeiffer mutation in an Apert patient: how wide is the spectrum of variability due to mutations in the FGFR2 gene? Am J Med Genet. 1997;71(2):243–5.
65. Passos-Bueno MR, Sertie AL, Richieri-Costa A, Alonso LG, Zatz M, Alonso N, Brunoni D, Ribeiro SFM. Description of a new mutation and characterization of *FGFR1*, *FGFR2*, and *FGFR3* mutations among Brazilian patients with syndromic craniosynostoses. Am J Med Genet. 1998;78(3):237–41.
66. Paumard-Hernandez B, Berges-Soria J, Barroso E, Rivera-Pedroza CI, Perez-Carrizosa V, Benito-Sanz S, Lopez-Messa E, Santos F, Garcia R II, Romance A, Ballesta-Martinez JM, Lopez-Gonzalez V, Campos-Barros A, Cruz J, Guillen-Navarro E, Sanchez Del Pozo J, Lapunzina P, Garcia-Minaur S, Heath KE. Expanding the mutation spectrum in 182 Spanish probands with craniosynostosis: identification and characterization of novel *TCF12* variants. Eur J Hum Genet. 2015;23(7):907–14.
67. Pollock PM, Gartside MG, Dejeza LC, Powell MA, Mallon MA, Cancer Genome Project, Davies H, Mohammadi M, Futreal PA, Stratton MR, Trent JM, Goodfellow PJ. Frequent activating FGFR2 mutations in endometrial carcinomas parallel germline mutations associated with craniosynostosis and skeletal dysplasia syndromes. Oncogene. 2007;26(50):7158–62.
68. Preston RA, Post JC, Keats BJ, Aston CE, Ferrell RE, Priest J, Nouri N, Losken HW, Morris CA, Hurtt MR, et al. A gene for Crouzon craniofacial dysostosis maps to the long arm of chromosome 10. Nat Genet. 1994;7(2):149–53.
69. Qin J, Calabrese P, Tiemann-Boege I, Shinde DN, Yoon SR, Gelfand D, Bauer K, Arnheim N. The molecular anatomy of spontaneous germline mutations in human testes. PLoS Biol. 2007;5(9):e224.
70. Rahbari R, Wuster A, Lindsay SJ, Hardwick RJ, Alexandrov LB, Turki SA, Dominiczak A, Morris A, Porteous D, Smith B, Stratton MR, UK10K Consortium, Hurles ME. Timing, rates and spectra of human germline mutation. Nat Genet. 2016;48(2):126–33.
71. Reardon W, Winter RM, Rutland P, Pulleyn LJ, Jones BM, Malcolm S. Mutations in the fibroblast growth factor receptor 2 gene cause Crouzon syndrome. Nat Genet. 1994;8(1):98–103.
72. Risch N, Reich EW, Wishnick MM, McCarthy JG. Spontaneous mutation and parental age in humans. Am J Hum Genet. 1987;41(2):218–48.
73. Robertson SC, Meyer AN, Hart KC, Galvin BD, Webster MK, Donoghue DJ. Activating mutations in the extracellular domain of the fibroblast growth factor receptor 2 function by disruption of the disulfide bond in the third immunoglobulin-like domain. Proc Natl Acad Sci USA. 1998;95(8):4567–72.
74. Rommens JM, Iannuzzi MC, Kerem B, Drumm ML, Melmer G, Dean M, Rozmahel R, Cole JL, Kennedy D, Hidaka N, et al. Identification of the cystic fibrosis gene: chromosome walking and jumping. Science. 1989;245(4922):1059–65.
75. Roscioli T, Elakis G, Cox TC, Moon DJ, Venselaar H, Turner AM, Le T, Hackett E, Haan E, Colley A, Mowat D, Worgan L, Kirk EP, Sachdev R, Thompson E, Gabbett M, McGaughran J, Gibson K, Gattas M, Freckmann ML, Dixon J, Hoefsloot L, Field M, Hackett A, Kamien B, Edwards M, Ades LC, Collins FA, Wilson MJ, Savarirayan R, Tan TY, Amor DJ, McGillivray G, White SM, Glass IA, David DJ, Anderson PJ, Gianoutsos M, Buckley MF. Genotype and clinical care correlations in craniosynostosis: findings from a cohort of 630 Australian and New Zealand patients. Am J Med Genet C Semin Med Genet. 2013;163C(4):259–70.
76. Rutland P, Pulleyn LJ, Reardon W, Baraitser M, Hayward R, Jones B, Malcolm S, Winter RM, Oldridge M, Slaney SF, Poole MD, Wilkie AOM. Identical mutations in the *FGFR2* gene cause both Pfeiffer and Crouzon syndrome phenotypes. Nat Genet. 1995;9(2):173–6.
77. Schuller AC, Ahmed Z, Ladbury JE. Extracellular point mutations in FGFR2 result in elevated ERK1/2 activation and perturbation of neuronal differentiation. Biochem J. 2008;410(1):205–11.

78. Shiang R, Thompson LM, Zhu YZ, Church DM, Fielder TJ, Bocian M, Winokur ST, Wasmuth JJ. Mutations in the transmembrane domain of FGFR3 cause the most common genetic form of dwarfism, achondroplasia. Cell. 1994;78(2):335–42.
79. Shin HR, Bae HS, Kim BS, Yoon HI, Cho YD, Kim WJ, Choi KY, Lee YS, Woo KM, Baek JH, Ryoo HM. PIN1 is a new therapeutic target of craniosynostosis. Hum Mol Genet. 2018;27(22):3827–39.
80. Shin HR, Kim BS, Kim HJ, Yoon H, Kim WJ, Choi JY, Ryoo HM. Excessive osteoclast activation by osteoblast paracrine factor RANKL is a major cause of the abnormal long bone phenotype in Apert syndrome model mice. J Cell Physiol. 2022;237(4):2155–68.
81. Shukla V, Coumoul X, Wang RH, Kim HS, Deng CX. RNA interference and inhibition of MEK-ERK signaling prevent abnormal skeletal phenotypes in a mouse model of craniosynostosis. Nat Genet. 2007;39(9):1145–50.
82. Tonne E, Due-Tonnessen BJ, Mero IL, Wiig US, Kulseth MA, Vigeland MD, Sheng Y, von der Lippe C, Tveten K, Meling TR, Helseth E, Heimdal KR. Benefits of clinical criteria and high-throughput sequencing for diagnosing children with syndromic craniosynostosis. Eur J Hum Genet. 2021;29(6):920–9.
83. Topa A, Rohlin A, Fehr A, Lovmar L, Stenman G, Tarnow P, Maltese G, Bhatti-Softeland M, Kolby L. The value of genome-wide analysis in craniosynostosis. Front Genet. 2023;14:1322462.
84. Tsai FJ, Tsai CH, Peng CT, Lin SP, Hwu WL, Wang TR, Lee CC, Wu JY. Molecular diagnosis of Apert syndrome in Chinese patients. Acta Paediatr Taiwan. 1999;40(1):31–3.
85. Vortkamp A, Gessler M, Grzeschik KH. GLI3 zinc-finger gene interrupted by translocations in Greig syndrome families. Nature. 1991;352(6335):539–40.
86. Wang Y, Xiao R, Yang F, Karim BO, Iacovelli AJ, Cai J, Lerner CP, Richtsmeier JT, Leszl JM, Hill CA, Yu K, Ornitz DM, Elisseeff J, Huso DL, Jabs EW. Abnormalities in cartilage and bone development in the Apert syndrome FGFR2$^{+/S252W}$ mouse. Development. 2005;132(15):3537–48.
87. Wang Y, Sun M, Uhlhorn VL, Zhou X, Peter I, Martinez-Abadias N, Hill CA, Percival CJ, Richtsmeier JT, Huso DL, Jabs EW. Activation of p38 MAPK pathway in the skull abnormalities of Apert syndrome *Fgfr2*$^{+P253R}$ mice. BMC Dev Biol. 2010;10:22.
88. Wilkie AOM. Bad bones, absent smell, selfish testes: the pleiotropic consequences of human FGF receptor mutations. Cytokine Growth Factor Rev. 2005;16(2):187–203.
89. Wilkie AOM. Cancer drugs to treat birth defects. Nat Genet. 2007;39(9):1057–9.
90. Wilkie AOM, Goriely A. Gonadal mosaicism and non-invasive prenatal diagnosis for 'reassurance' in sporadic paternal age effect (PAE) disorders. Prenat Diagn. 2017;37(9):946–8.
91. Wilkie AOM, Morriss-Kay GM, Jones EY, Heath JK. Functions of fibroblast growth factors and their receptors. Curr Biol. 1995;5(5):500–7.
92. Wilkie AOM, Slaney SF, Oldridge M, Poole MD, Ashworth GJ, Hockley AD, Hayward RD, David DJ, Pulleyn LJ, Rutland P, et al. Apert syndrome results from localized mutations of *FGFR2* and is allelic with Crouzon syndrome. Nat Genet. 1995b;9(2):165–72.
93. Wilkie AOM, Patey SJ, Kan SH, van den Ouweland AMW, Hamel BCJ. FGFs, their receptors, and human limb malformations: clinical and molecular correlations. Am J Med Genet. 2002;112(3):266–78.
94. Yang F, Whelan EC, Guan X, Deng B, Wang S, Sun J, Avarbock MR, Wu X, Brinster RL. FGF9 promotes mouse spermatogonial stem cell proliferation mediated by p38 MAPK signalling. Cell Prolif. 2021;54(1):e12933.
95. Yin L, Du X, Li C, Xu X, Chen Z, Su N, Zhao L, Qi H, Li F, Xue J, Yang J, Jin M, Deng C, Chen L. A Pro253Arg mutation in fibroblast growth factor receptor 2 (Fgfr2) causes skeleton malformation mimicking human Apert syndrome by affecting both chondrogenesis and osteogenesis. Bone. 2008;42(4):631–43.
96. Yoon SR, Qin J, Glaser RL, Jabs EW, Wexler NS, Sokol R, Arnheim N, Calabrese P. The ups and downs of mutation frequencies during aging can account for the Apert syndrome paternal age effect. PLoS Genet. 2009;5(7):e1000558.
97. Yoon WJ, Cho YD, Kim WJ, Bae HS, Islam R, Woo KM, Baek JH, Bae SC, Ryoo HM. Prolyl isomerase Pin1-mediated conformational change and subnuclear focal accumulation of Runx2 are crucial for fibroblast growth factor 2 (FGF2)-induced osteoblast differentiation. J Biol Chem. 2014;289(13):8828–38.
98. Yu K, Ornitz DM. Uncoupling fibroblast growth factor receptor 2 ligand binding specificity leads to Apert syndrome-like phenotypes. Proc Natl Acad Sci USA. 2001;98(7):3641–3.
99. Zhang J, Li J, Saucier JB, Feng Y, Jiang Y, Sinson J, McCombs AK, Schmitt ES, Peacock S, Chen S, Dai H, Ge X, Wang G, Shaw CA, Mei H, Breman A, Xia F, Yang Y, Purgason A, Pourpak A, Chen Z, Wang X, Wang Y, Kulkarni S, Choy KW, Wapner RJ, Van den Veyver IB, Beaudet A, Parmar S, Wong LJ, Eng CM. Non-invasive prenatal sequencing for multiple Mendelian monogenic disorders using circulating cell-free fetal DNA. Nat Med. 2019;25(3):439–47.